Interleukin-15 enhances cellular proliferation and up-regulates CNS homing molecules in pre-B acute lymphoblastic leukaemia

Mark TS Williams[1], Yasar Yousafzai[1,2], Charlotte Cox[3], Allison Blair[3,4], Ruaidhrí Carmody[1], Shuji Sai[5], Karen E Chapman[5], Rachel McAndrew[6], Angela Thomas[6], Alison Spence[7], Brenda Gibson[7], Gerard J Graham[1], Christina Halsey*[1,7].

[1] Centre for Immunobiology, Institute of Infection, Immunity and Inflammation, College of Medical, Veterinary and Life Sciences, University of Glasgow, UK

[2] Khyber Medical University, Hayatabad, Peshawar, Pakistan.

[3] Bristol Institute for Transfusion Sciences, National Health Service Blood and Transplant, Filton, Bristol, UK

[4] School of Cellular and Molecular Medicine, University of Bristol, UK.

[5] Endocrinology Unit, Centre for Cardiovascular Sciences, The Queen's Medical Research Institute, University of Edinburgh, Edinburgh, UK

[6] Department of Paediatric Haematology, Royal Hospital for Sick Children, Edinburgh, UK

[7] Department of Paediatric Haematology, Royal Hospital for Sick Children, Yorkhill, Glasgow, UK

* Address for correspondence: Dr Christina Halsey, Centre for Immunobiology, Institute of Infection, Immunity and Inflammation, College of Medical, Veterinary and Life Sciences, University of Glasgow. Email: chris.halsey@glasgow.ac.uk, telephone +44 141 3308135, Fax +44 141 3304297.

Running Title: Mechanisms of IL-15 in ALL

Text word count: 3965 words

Abstract word count: 200 words

Number of figures and tables: 7

Number of references: 50

Key Points:

1. IL-15 has been implicated in central nervous system disease and leukaemogenesis but the biological mechanisms are unknown.
2. IL-15 increases pre-B ALL growth and up-regulates CNS homing molecules. MEK/ERK, PI3K and NFκB inhibitors block IL-15 growth effects.

ABSTRACT

Genome-wide association studies and transcriptomics have consistently implicated the interleukin-15 (IL-15) gene in acute lymphoblastic leukaemia (ALL) biology, including associations with disease susceptibility, resistance to initial therapy and increased risk of mediastinal and central nervous system (CNS) involvement. However, whether pre-B ALL blasts directly respond to IL-15 is currently unknown. Here we show that the majority of pre-B ALL primary samples and cell lines express IL-15 and all 3 components of its heterotrimeric receptor and that primary pre-B ALL cells show increased growth in culture in response to IL-15. Investigation of mechanisms of action using highly IL-15 responsive SD-1 cells shows this growth advantage is maximal under low serum conditions, mimicking those found in cerebrospinal fluid. Addition of IL-15 also up-regulates PSGL-1 and CXCR3, molecules associated with lymph-node and CNS trafficking. Investigation of downstream signalling pathways indicates that IL-15 induces STAT5, ERK1/2 and to a lesser extent PI3K and NFκB phosphorylation. The IL-15 mediated growth advantage is abolished by MEK/ERK, PI3K and NFκB inhibitors, but preserved in the presence of STAT5 inhibition. Together these observations provide a plausible mechanistic link between increased levels of IL-15 expression and leukaemogenesis, high-risk disease, mediastinal involvement and CNS relapse and suggest potential therapeutic targets.

INTRODUCTION

Large-scale unbiased genomic approaches are increasingly used in leukaemia research to identify factors that influence tumourigenesis, biological features and/or response to therapy. Genetic "hits" identified by these investigations may be directly involved in the disease or bystanders incidentally-linked to other (often unknown) genetic loci that drive the process. For this reason it is important to verify the biological role of implicated genes if progress is to be made. Several large observational studies have linked interleukin-15 (IL-15) single-nucleotide polymorphisms (SNPs) or mRNA levels to aspects of acute lymphoblastic leukaemia (ALL) biology. Two independent genome-wide association studies (GWAS) identified polymorphisms in the IL-15 gene as predictors of leukaemia development[1] and resistance to initial therapy[2]. Microarray data suggest that IL-15 mRNA levels predict the likelihood of central nervous system (CNS) relapse in childhood ALL[3]. Finally, a clinical study looking at IL-15 mRNA in adult ALL showed that higher IL-15 expression was associated with mediastinal and lymph node (LN) infiltration but not hepatosplenomegaly (rates of CNS involvement were not reported)[4]. Importantly some IL-15 SNPs correlate with increased promoter activity when tested in reporter constructs[5], suggesting a possible direct link to pathogenesis. However, the mechanisms underlying any biological advantage for high IL-15 expression in ALL are currently unknown.

IL-15 is a pleiotropic cytokine sharing structural homology and receptor components with interleukin-2 (IL-2)[6,7]; together these cytokines play pivotal roles in regulatory and effector functions of the normal immune system. IL-15 influences proliferation, differentiation, resistance to apoptosis[8] and cellular localization of T[9] and B lymphocytes[10], neutrophils[11] and natural killer (NK) cells[12]. A possible role for IL-15 in malignant disorders of the immune system was first suggested by its identification in an Adult T-cell Leukaemia-Lymphoma (ATLL) cell line[13] and the fact that IL-15 transgenic mice develop an NK/T large granular lymphocyte leukaemia (LGL) like disease[14,15]. IL-15 stimulates proliferation of primary T-ALL blasts in culture[16] and chronic

exposure of normal LGLs to IL-15 induces leukaemic transformation[17]. Links to B-cell malignancies – myeloma[18] and CLL[19,20] have also been reported.

The IL-15 gene is expressed in many tissues including the central nervous system[21,22]. Two IL-15 isoforms encode the same mature IL-15 protein but with different signal peptides determining cellular localisation[23]. The 21 amino-acid short-signal peptide isoform (SSP-IL-15) is targeted to the cytoplasm – its function remains largely unknown. In contrast, the 48 amino-acid long-signal peptide isoform (LSP-IL-15) targets IL-15 for presentation on the cell-surface and/or secretion. IL-15 signals via a heterotrimeric receptor complex comprising a common γ chain, an IL-2/IL-15Rβ chain[6] and a specific IL-15Rα chain[24]. This IL-15Rα chain binds IL-15 with high-affinity (1000 fold higher than IL-2/IL-2Rα interactions[24]) and can be secreted or membrane bound. IL-15/IL-15Rα heterodimers may be the main active form of IL-15 in human serum[25]. Thus, IL-15 can be presented in *cis* or *trans* and act in an autocrine, paracrine or juxtacrine fashion. It is unknown whether the reported associations between IL-15 SNPs and ALL reflect a direct biological role for IL-15 in ALL. If so, this could be due to direct effects of IL-15 on leukaemic blasts or indirect effects via IL-15 modulation of the immune system or a combination of the two.

In this study we investigate the biological effect of IL-15 in pre-B ALL. We show that IL-15 is expressed by pre-B ALL blasts, which respond to both autocrine and paracrine IL-15 signalling. We show that the growth advantage of leukaemic blasts exposed to IL-15 is maximal under low-serum conditions and identify downstream pathways responsible for the growth advantage. Thus, we have identified possible therapeutic targets that could be used to treat high-risk disease and/or CNS relapse.

MATERIALS AND METHODS

Cell culture and primary cells

Human ALL cell lines SD-1, REH, Molt-4, Sup-B15, SEM and CCRF-CEM were maintained in RPMI supplemented with 10% FBS and 1% Penicillin/Streptomycin (Invitrogen). Pre-B ALL primary samples were obtained from the Leukaemia Lymphoma Research Childhood Leukaemia Cellbank and from our local institutions. Cells used for receptor expression analysis were cultured in complete RPMI, at 37^{o}C, 5% CO_2 for 24h before harvesting in Trizol (Invitrogen). Primary cells were processed and cryopreserved as previously described[26]. For growth curves, primary cells were thawed and set up in suspension culture in HP01 media (Macopharma) supplemented with rhIL-3 (20ng/ml), rhIL-7 (20ng/ml) and rhSCF(50ng/ml) (3-cytokine mix) (all R&D systems)[27]. After 7-14 days in culture (recovery time) these cells were washed and split in to two conditions: 3-cytokine mix only or 3-cytokine mix + rhIL-15 (25ng/ml) (Peprotech). Cells were maintained over a 3-week period with weekly half-media changes. Viability and absolute cell counts (live lymphoid blasts) were determined using a MACSQuant flow cytometer (Miltenyi Biotec) after staining with 7-Aminoactinomycin-D (Invitrogen). Patient's details are given in supplementary table 1. This project was approved by the West of Scotland Research Ethics Committee.

Xenotransplants

NOD.Cg-*Prkdc*^{scid}*Il2rg*^{tm1Wjl}/SzJ (NSG) breeders were obtained from Charles River, Europe and the colony maintained at the Central Research Facility, University of Glasgow. Mice were kept in sterile isolators with autoclaved food, bedding and water. At 6-8 weeks of age mice were injected intravenously with 1x10^6 leukaemic cells via tail vein. Mice were sacrificed at 6 weeks post-injection or earlier if unwell. All animal experiments were approved by the University of Glasgow Ethical Review Process Committee.

Histology

Murine brains were fixed in 10% neutral-buffered formalin and paraffin embedded. Haematoxylin and Eosin staining (Sigma) was performed on 5µm

brain sections. Anti-CD45 immunohistochemistry used standard protocols; paraffin-embedded sections were dewaxed and hydrated prior to antigen retrieval at 100^0C for 15 minutes in 0.01 mol/L citrate buffer, pH 6.0. Following blocking in 20% horse serum/PBS-Tween20 (0.05%) (PBST) with avidin block, sections were incubated with mouse anti-human CD45 antibody/isotype control antibody (mouse IgG1) (Dako) and horse, biotinylated anti-mouse – secondary antibody (Vector Laboratories) with biotin block. Sections were treated with ABC kit (Vector Laboratories) and DAB to visualise antibody binding. All imaging was performed on an Axiostar plus microscope and images were acquired using Axiovision Rel 4.2 software (Carl Zeiss, Oberkochen Germany)

PCR

Total RNA was extracted using an RNeasy kit (Qiagen) or following homogenization in Trizol. All samples underwent DNase digestion (RNase-free DNase, Qiagen). RNA (200ng) was reverse-transcribed using random primers and AffinityScript reverse transcriptase (Stratagene). RT-PCR used standard cycling conditions on an Applied Biosystems Veriti thermal cycler. Primary cell IL-15 qPCR was performed using PerfeCTa SYBR Green FastMix, ROX (Quanta Biosciences). Primers were designed using Primer3 software. IL-15R quantitative PCR used Taqman primers and probes with Universal Mastermix (Applied Biosystems). Custom designed Taqman low density arrays (TLDA) were run as previously described[28]. Data were analysed using RQ Manager 1.2.4 software (Applied Biosystems). The RT^2 Human tumour metastasis profiler arrays (Catalogue number PAHS-028ZC-2) (SABiosciences) were run using SYBR green ROX qPCR Mastermix (SABiosciences) according to the manufacturer's instructions. All qPCR reactions were performed using the Applied Biosystems 7500/7900HT Real-PCR System. PCR primer details and assay IDs are listed in supplementary table 2.

Flow cytometry and Annexin V assays

CXCR3 and PSGL-1 antibodies were obtained from Ebioscience. Intracellular IL-15 was detected using anti-human IL-15-PE antibodies/isotype control

198 (R&D systems) following fixation and permeabilization using BD
199 Cytofix/Cytoperm (BD Biosciences) according to the manufacturer's
200 instructions. Apoptosis was determined via the Annexin V apoptosis detection
201 kit FITC (Ebioscience) according to the manufacturer's instructions. Data were
202 acquired on a MACSQuant flow cytometer (Miltenyi Biotec) and results were
203 analysed using FlowJo7.2.4 software (Tree Star Inc, OR, USA).
204
205 *Western blotting*
206 Cells were lysed in RIPA buffer (Sigma) with protease/phosphatase cocktail
207 inhibitor (1:100 dilution – Sigma). 10 μg total protein (determined using a BCA
208 protein assay kit, Thermoscientific) was run on a 12% bis-tris gel (Invitrogen)
209 and transferred via iBlot (Invitrogen) to nitrocellulose membrane. Blocking was
210 performed in 10% non-fat milk (0.05% Tween/PBS). All antibodies were
211 purchased from New England Biolabs and used at 1:1000 dilutions unless
212 otherwise stated. Chemiluminescence was detected using West Femto super
213 signal (Thermoscientific).
214
215 *SD-1 Growth curves and inhibitors*
216 SD-1 and Sup-B15 cells were seeded into 24 well flat bottom plates at 1.5 x
217 10^5 cells/ml. Viable cells were counted using a haemocytometer with trypan-
218 blue dead-cell exclusion. Cells were exposed to IL-15Rα neutralizing antibody
219 (nAb) (R & D Systems), isotype control antibody (R & D Systems), or rhIL-15.
220 Small molecule inhibitors of signalling pathways were diluted in DMSO and
221 added to cells with or without addition of 25ng/ml IL-15 and growth was
222 compared to cells grown in the same percentage of DMSO (vehicle controls).
223 Cell division was assessed using the CellTrace Violet proliferation kit
224 (Invitrogen) using colcemid treated cells as a non-dividing control[29].
225
226 *MTT assays*
227 120 μl of MTT (5 mg/ml) (Sigma) in PBS was added to each well of 24-well
228 plates containing SD-1 cells and incubated for 4 h at 37 °C. Following
229 centrifugation and removal of supernatant, 600 μl of extraction reagent (Fisher
230 Scientific) was added per well and agitated for 15mins. 100 μl solution/well

was then transferred to a 96-well plate and absorbance measured in a sunrise absorbance reader (Tecan) at 570 nm (background wavelength 660 nm). Analysis used MagellanCE6 software (Tecan).

Statistics

Parametric data were analysed using Student's unpaired t-tests. Non-parametric data were analysed using Mann-Whitney (2 groups, unpaired), Kruskal-Wallis (>2 groups, unpaired) or Wilcoxon matched-pairs sign rank (>2 groups, paired) tests. A p-value of ≤0.05 was considered significant. All analysis was carried out using GraphPad Prism software (La Jolla, CA).

RESULTS

Leukaemic blasts express IL-15 and IL-15 receptors and levels correlate with CNS infiltration in xenografts.

RT-PCR was used to investigate expression of the two IL-15 isoforms and three IL-15 receptor subunits in pre-B ALL cell lines; SD-1, Sup-B15, REH and SEM, and 19 primary pre-B leukaemic diagnostic samples (patient and cell line details; Supplementary Table 1). All expressed the cell-surface/secreted LSP-IL-15 isoform, but expression of the cytoplasmic SSP-IL-15 isoform was only detected in 6/19 primary samples (Figure 1a and Supplementary Table I). In addition, all samples expressed IL-15Rα and the common γ chain and 14/17 primary samples expressed IL-15Rβ (Figure 1a). This suggests that the majority of ALL cells have the potential to secrete and respond to IL-15 using autocrine, juxtacrine or paracrine signalling loops.

Quantitative PCR indicates that primary ALL samples show a spectrum of IL-15 mRNA expression (Figure 1b). High expression has been shown to predict cytospin positive CNS disease at diagnosis and the risk of CNS relapse[3]. To examine the link with CNS disease further we used a xenograft model to investigate CNS infiltration by pre-B cell lines. All cell lines tested were capable of CNS infiltration (Figure 1c) but with different kinetics as measured by time to hind-limb paralysis (HLP), a surrogate marker for leukaemic infiltration of the leptomeninges (Figure 1d). Higher expression levels of

mRNA encoding IL-15 and all 3 components of the IL-15 receptor (Figure 1e-h) were associated with shorter time to HLP (Figure 1d).

Pre-B ALL cells can respond directly to IL-15

To test whether IL-15 mediates direct effects on pre-B ALL cells, 6 primary samples (patient details in supplementary table 1) and 4 pre-B ALL cell lines (SD-1, Sup-B15, REH and SEM) were exposed to IL-15 in suspension culture and the effects on growth were examined. Five of six primary samples (Figure 2a) showed increased cell numbers in the presence of IL-15. To account for the wide variation in starting cell numbers and differing rates of proliferation between primary samples we also calculated fold change in cell numbers compared to baseline (Figure 2b) – this confirmed that IL-15 significantly enhanced cell growth when added to standard 3-cytokine mix. The effect of IL-15 on cell lines is more restricted and is shown in Figure 2c, SD-1 cells show a dose-dependent response to exogenous IL-15 but other cell lines appear to be IL-15 independent. To investigate whether endogenous IL-15 also plays a role, cells were incubated with an IL-15Rα nAb (in the absence of an exogenous source of IL-15) to block autocrine IL-15 signalling but leave signalling from IL-2 (which uses the same beta/gamma receptor subunit) and other cytokines (that use the common gamma chain) unaffected. Exposure of to IL-15Rα nAbs significantly decreased cell number at both 72 and 96 h in SD-1 but not Sup-B15 cells (Figure 2d).

These experiments show that pre-B ALL samples can respond directly to addition of IL-15 in culture resulting in increased growth.

Mechanism of action of IL-15 in promoting pre-B ALL growth.

To investigate the mechanism of IL-15 action on pre-B ALL blasts, Sup-B15 and SD-1 cells were studied further, since they carry the same leukaemic translocation – t(9;22) *BCR-ABL* - but differ markedly in their IL-15 expression levels and speed of onset of CNS disease; high in SD-1 cells and low in Sup-B15 cells (Figure 1d).

IL-15 protein is difficult to detect due to its highly controlled secretion and fast turnover[25,30]. Consistent with previous reports[18] IL-15 secretion was undetectable using ELISA (sensitivity ≥8pg/ml, data not shown). However, intracellular IL-15 protein was detectable by flow cytometry in SD-1 cells, with lower levels in Sup-B15 (Figure 3a). Western blotting confirmed all three IL-15 receptor components are expressed by both cell lines with higher levels of IL-15Rα in SD-1 than Sup-B15 (Figure 3b).

The observed increased cell numbers in the presence of IL-15 (Figure 2) could reflect reduced apoptosis or an ability to withstand growth arrest under conditions of serum depletion. IL-15 has powerful anti-apoptotic effects in T and B cells[8,31]. Therefore we investigated whether IL-15 affected apoptosis in SD-1 cells. There was no alteration in BCL-xL and BCL-2 levels (Figure 3c) and no differences in apoptosis between IL-15 and untreated SD-1 cells measured by PARP cleavage (Figure 3d), Annexin V staining (Figure 3e) or caspase-3 cleavage (supplementary figure 1a). To uncover a potential anti-apoptotic role for IL-15 in the context of induced apoptotic stress, SD-1 cells were treated with dexamethasone (100 nM, 1 μM and 10 μM) for 48 hours to induce apoptosis. Dexamethasone had no effect on SD-1 apoptosis or viability, assessed using Annexin V (Figure 3f) and MTT (Figure 3g) respectively. Importantly, this could not be overcome by treatment with IL-15Rα nAb (Figure 3h) suggesting that IL-15-IL-15Rα signalling is not responsible for the resistance of SD-1 cells to dexamethasone-induced apoptosis.

Together these findings argue against reduced apoptosis being responsible for the higher plateau in IL-15 treated SD-1 cells. An alternative explanation is that IL-15 prevents growth arrest under conditions of serum depletion (as seen after 72-96 hours in culture without replenishment of growth media). To test this, SD-1 and Sup-B15 cells were grown under no/low serum conditions with or without IL-15. IL-15 significantly enhanced the proliferation of SD-1 cells growing under conditions of no serum, 1% and 2.5% serum (Figure 4a, b and supplementary Figure 1). Maximal benefit (in terms of percentage

increase in growth with IL-15 treatment) was seen with 0% and 1% serum conditions (figure 4b and c). Sup-B15 cells showed no response (Figure 4c). Again there was no evidence that the IL-15 growth advantage was due to rescue from apoptosis (Figure 4d and supplementary figure 1).

Thus, IL-15Rα neutralisation reduces, and exogenous IL-15 stimulates, proliferation of SD-1 cells. These effects are not mediated via alterations in apoptosis. The significant growth advantage conferred by IL-15 treatment under low serum conditions provides a potential explanation for the association between high IL-15 expression and leukaemia relapse in the low-protein environment of the CNS.

IL-15 is not directly chemotactic but up-regulates PSGL1, CXCR3 and SERPINE1.

In addition to its growth effects, IL-15 could play a role in leukocyte trafficking either acting as a chemoattractant[32,33] or by modulating homing[34,35]. Since IL-15 is expressed in the CNS[21,22] we tested whether IL-15 affected chemotaxis of SD-1 cells but were unable to show any migration towards an IL-15 gradient (Figure 5a). To investigate whether IL-15 indirectly regulates cellular migration or metastasis, two expression arrays were performed on IL-15 treated SD-1 cells. Firstly, a Taqman low density array of 30 human chemokine receptors, integrins and selectins examined whether IL-15 treatment up-regulated known leukocyte homing molecules. Only 2 out of 30 genes showed significant up-regulation (Supplementary Figure 2): the chemokine receptor, *CXCR3* and the selectin ligand, platelet selectin glycoprotein ligand-1 (PSGL-1/*SELPLG*). Interestingly, both are implicated in blood-CSF barrier transit[36,37]. These findings were confirmed by qPCR on an independent set of samples (Figure 5b) and up-regulation of PSGL-1 was also seen by flow cytometry (Figure 5c). We went on to show that leukaemic cells can migrate towards the CXCR3 ligand CXCL10 and that CXCL10 is detectable in CSF samples from patients with ALL. In addition, we show that the PSGL-1 receptor P-selectin is expressed on meningeal post-capillary venules in NSG mice (supplementary figure 3).

A second approach involved a RT^2 PCR profiler array investigating 96 genes implicated in human tumour metastasis. IL-15 treatment had only a modest effect with just 7 genes showing greater than 2-fold up- or down-regulation (Figure 5d). Independent validation by qPCR confirmed that *SERPINE1* was significantly, although modestly, up-regulated by IL-15 treatment (Figure 5e and supplementary figure 4).

Together these experiments suggest that high IL-15 may increase interactions of circulating ALL cells with the blood-CSF and blood-LN barriers (via PSGL1/CXCR3) and/or promote invasiveness via SERPINE1 expression.

IL-15 induces STAT5 and ERK1/2 phosphorylation

Finally we investigated downstream signalling pathways that might mediate the effects of IL-15 in ALL using phospho-specific antibodies for ERK1/2, STAT5, IκBα and Akt. Strong phosphorylation of STAT5 and ERK1/2 was seen within 15 minutes of addition of IL-15 to SD-1 cells (Figure 6a-c). In addition, some activation of the NFκB and PI3K-Akt pathways is suggested by minor increases in phopsho-IκBα and phospho-Akt although these pathways are also constitutively activated in these cells (Figure 6a, 6d).

Given the potential therapeutic benefit of blocking IL-15 signalling in ALL, small molecule inhibitors were investigated. Use of an ERK1/2 inhibitor (FR180204, Calbiochem) completely abolished the growth advantage conferred by IL-15 (Figure 7a). In contrast, STAT5 inhibition (573108, Calbiochem) reduced overall growth although the growth advantage of exogenous IL-15 was still maintained (Figure 7b and supplementary figure 5). A more potent MEK inhibitor (U0126, Calbiochem), which lies upstream of ERK1/2 in the Raf/Ras/ERK pathway, profoundly reduced the growth of SD-1 cells and abolished any IL-15 stimulation of growth (Figure 7c and supplementary figure 5). Both PI3Kinase (LY 294002, Calbiochem) and NFκB (IKK-2 inhibitor IV, Calbiochem) inhibitors had profound effects on leukaemic cell growth both with and without IL-15 (figure 7d) making assessment of their specific role in IL-15 signalling difficult.

Together these results suggest that the Raf/Ras/ERK signalling pathway is directly involved in mediating IL-15 growth promoting effects whereas STAT5 does not seem to play a role in this pathway. PI3K and NFκB may also be important either directly or indirectly in IL-15 action.

DISCUSSION

Here we have shown that IL-15 up-regulates leukocyte trafficking molecules and promotes cell proliferation under normal and hostile conditions in pre-B ALL. Thus we have established a mechanistic link between the effects of IL-15 on leukaemic blasts and GWAS and microarray studies identifying IL-15 as a candidate gene for leukaemia development[1], high-risk MRD[2] and CNS relapse[3].

The GWAS data[1,2] associate germline SNPs in IL-15 with leukaemia and therefore cannot distinguish the production of IL-15 by leukaemic blasts themselves or by the host microenvironment as the most important determinant of biological response. We show evidence for both; inhibition of autocrine or juxtacrine signalling via IL-15Rα neutralization reduced the growth of SD-1 cells, but larger growth-promoting effects were seen with exogenous IL-15, suggesting that paracrine signalling from the host microenvironment may be more important than autocrine signalling from the blasts themselves. All primary samples express IL-15 but a few samples lack expression of all components of the IL-15 receptor. This suggests that there may be heterogeneity between patients in the ability to respond to IL-15. Associations between IL-15 receptor expression and disease outcome have never been tested. Our sample size is too small to address this important question, but study of a larger cohort of patients could potentially identify patients that would benefit from blockade of IL-15 receptor signalling using pharmacological inhibitors as discussed below.

High IL-15 expression in primary leukaemic blasts is correlated with CNS disease[3]. Leukaemic deposits in the CNS grow within the leptomeninges

bathed in CSF. CSF has a very low protein content[38], a condition under which we show the growth enhancement effect of IL-15 is particularly marked. IL-15 can promote survival in serum-free conditions in NK cells[12] although in that case the effect was mediated via prevention of apoptosis rather than proliferation. We hypothesize that high levels of IL-15 facilitate engraftment and long term survival in the CNS. IL-15 may be more important in the CNS microenvironment than in the BM where serum-starvation is unlikely to be a major selective pressure. Importantly IL-15 is produced in the CNS by glial cells[22] and high levels of IL-15 are associated with neuro-inflammatory disorders such as multiple sclerosis[21], suggesting that IL-15 may be of particular importance in brain pathology.

In addition to local effects on cell proliferation and survival, IL-15 may facilitate extramedullary dissemination of ALL, promoting bulky mediastinal and LN disease[4] and CNS relapse[3]. IL-15 is directly chemotactic to T cells[32,33] and NK cells[39] and also indirectly influences leukocyte trafficking. IL-15Rα knockout mice have low numbers of circulating T and B cells and fewer leukocytes in lymph nodes, despite grossly normal B and T cell development[35]. IL-15 also plays a part in the regulation of immature B cell homing via modulation of IFNγ mediated homing pathways[34]. The induction of PSGL-1 by IL-15 may alter leukocyte trafficking; PSGL-1 is a ligand for both L and P selectins, the major determinants of tethering and rolling in LN endothelial venules[40]. In addition, P-selectin/PSGL-1 interactions are important determinants of cellular passage across the blood-CSF barrier[36]. Our screen also identified the chemokine receptor CXCR3 and the protease SERPINE1 as inducible by IL-15. CXCR3 is highly expressed in CSF leucocytes and its ligand CXCL10 is up-regulated in the CSF of multiple sclerosis patients[41], suggesting that CXCR3 may be important in CNS cell-entry. SERPINE1 is a serine protease inhibitor that inhibits apoptosis[42] and plays important roles in cellular invasion and angiogenesis[43]. It is associated with poor prognosis in a variety of cancers[44]. Interestingly the gene encoding SERPINE1 is a known ERK1/2 target[45].

IL-15 induces phosphorylation of ERK1/2 and STAT5. Interestingly, both these signalling pathways are implicated in ALL pathogenesis. Constitutive activation of the Raf/Ras/MEK/ERK pathway is common in childhood ALL and acquired Ras mutations are considered to be driver mutations[46]. STAT5 activation is strongly associated with high-risk ALL subsets such as Philadelphia positive ALL[47] and "Philadelphia-like" ALL[48], both of which are associated with high-risk MRD and relapse. The growth advantage conferred by IL-15 is completely blocked by inhibition of ERK1/2. In contrast, STAT5 inhibition reduces overall leukaemic cell growth but does not abolish the growth-promoting effects of IL-15 suggesting it may play a role in other, as yet unidentified mechanisms, related to disease aggressiveness. The specific role of the PI3K/Akt pathways and NFκB pathways needs further investigation – our results show that inhibition of these pathways abrogates IL-15 growth effects but due to the requirement for these pathways for basal leukaemic cell growth in culture further analysis will be required to determine whether these effects are direct or indirect.

Finally, it is worth noting that IL-15 may also influence the immune response to ALL. Administration of IL-15 has been suggested as a potential cancer treatment by boosting anti-tumour immune responses[49]. Although our studies did not address the effects of IL-15 on host immune cells, our findings, along with others[18-20], suggest that in ALL the increased malignant cell biological-fitness associated with high IL-15 might out-compete an increased immune response. Whether IL-15 has similar effects on growth of non-haematological malignancies is currently unknown, although IL-15 SNPs have also been linked to colon cancer[50].

Importantly, this paper illustrates how high-throughput unbiased approaches such as GWAS and microarray data can lead to focused studies investigating key biological drivers of disease that can be exploited by drug therapy. Our study provides not only an insight into mechanisms by which IL-15 promotes leukaemic cell growth and a propensity for LN and CNS involvement but also identifies potential drug targets.

ACKNOWLEDGMENTS

We thank the Leukaemia and Lymphoma Research Childhood Leukaemia Cell Bank and all contributing centres and patients. We thank E.Cosimo and A.Michie for help with cell division analysis, V.Kelly, P.Diamanti, J.Moppett, M.Cummins, H Blair and J.Vormoor for help with primary samples, O.Heidenreich and V.Saha for supply of cell lines. CH holds a Scottish Senior Clinical Fellowship (Scottish Funding Council). This work was supported by the Kay Kendall Leukaemia Fund (KKL454), RHSC, Edinburgh Haematology Fund and the Chief Scientist Office (SCD/08). GJG holds an MRC programme grant (G0901113).

AUTHORSHIP CONTRIBUTIONS

CH, GG, AB and RC designed the research and analysed the data, CH, MW, YY, CC, AB and SS performed the research. KC, RM, AT, AS and BG provided patient data and material. All authors contributed to writing of the manuscript.

DISCLOSURE OF CONFLICTS OF INTEREST

The authors have no conflicts of interest to declare

REFERENCES

1. Lin D, Liu C, Xue M, et al. The role of interleukin-15 polymorphisms in adult acute lymphoblastic leukemia. *PLoS One*. 2010;5(10):e13626.
2. Yang JJ, Cheng C, Yang W, et al. Genome-wide interrogation of germline genetic variation associated with treatment response in childhood acute lymphoblastic leukemia. *JAMA*. 2009;301(4):393-403.
3. Cario G, Izraeli S, Teichert A, et al. High interleukin-15 expression characterizes childhood acute lymphoblastic leukemia with involvement of the CNS. *J Clin Oncol*. 2007;25(30):4813-4820.
4. Wu S, Fischer L, Gokbuget N, et al. Expression of interleukin 15 in primary adult acute lymphoblastic leukemia. *Cancer*. 2010;116(2):387-392.
5. Zhang XJ, Yan KL, Wang ZM, et al. Polymorphisms in interleukin-15 gene on chromosome 4q31.2 are associated with psoriasis vulgaris in Chinese population. *J Invest Dermatol*. 2007;127(11):2544-2551.
6. Giri JG, Ahdieh M, Eisenman J, et al. Utilization of the beta and gamma chains of the IL-2 receptor by the novel cytokine IL-15. *EMBO J*. 1994;13(12):2822-2830.

7. Dobbeling U, Dummer R, Laine E, Potoczna N, Qin JZ, Burg G. Interleukin-15 is an autocrine/paracrine viability factor for cutaneous T-cell lymphoma cells. *Blood*. 1998;92(1):252-258.
8. Bulfone-Paus S, Ungureanu D, Pohl T, et al. Interleukin-15 protects from lethal apoptosis in vivo. *Nat Med*. 1997;3(10):1124-1128.
9. Grabstein KH, Eisenman J, Shanebeck K, et al. Cloning of a T cell growth factor that interacts with the beta chain of the interleukin-2 receptor. *Science*. 1994;264(5161):965-968.
10. Armitage RJ, Macduff BM, Eisenman J, Paxton R, Grabstein KH. IL-15 has stimulatory activity for the induction of B cell proliferation and differentiation. *J Immunol*. 1995;154(2):483-490.
11. Girard D, Paquet ME, Paquin R, Beaulieu AD. Differential effects of interleukin-15 (IL-15) and IL-2 on human neutrophils: modulation of phagocytosis, cytoskeleton rearrangement, gene expression, and apoptosis by IL-15. *Blood*. 1996;88(8):3176-3184.
12. Carson WE, Fehniger TA, Haldar S, et al. A potential role for interleukin-15 in the regulation of human natural killer cell survival. *J Clin Invest*. 1997;99(5):937-943.
13. Burton JD, Bamford RN, Peters C, et al. A lymphokine, provisionally designated interleukin T and produced by a human adult T-cell leukemia line, stimulates T-cell proliferation and the induction of lymphokine-activated killer cells. *Proc Natl Acad Sci U S A*. 1994;91(11):4935-4939.
14. Fehniger TA, Suzuki K, Ponnappan A, et al. Fatal leukemia in interleukin 15 transgenic mice follows early expansions in natural killer and memory phenotype CD8+ T cells. *J Exp Med*. 2001;193(2):219-231.
15. Yokohama A, Mishra A, Mitsui T, et al. A novel mouse model for the aggressive variant of NK cell and T cell large granular lymphocyte leukemia. *Leuk Res*. 2010;34(2):203-209.
16. Barata JT, Keenan TD, Silva A, Nadler LM, Boussiotis VA, Cardoso AA. Common gamma chain-signaling cytokines promote proliferation of T-cell acute lymphoblastic leukemia. *Haematologica*. 2004;89(12):1459-1467.
17. Mishra A, Liu S, Sams GH, et al. Aberrant overexpression of IL-15 initiates large granular lymphocyte leukemia through chromosomal instability and DNA hypermethylation. *Cancer Cell*. 2012;22(5):645-655.
18. Tinhofer I, Marschitz I, Henn T, Egle A, Greil R. Expression of functional interleukin-15 receptor and autocrine production of interleukin-15 as mechanisms of tumor propagation in multiple myeloma. *Blood*. 2000;95(2):610-618.
19. Trentin L, Cerutti A, Zambello R, et al. Interleukin-15 promotes the growth of leukemic cells of patients with B-cell chronic lymphoproliferative disorders. *Blood*. 1996;87(8):3327-3335.
20. de Totero D, Meazza R, Capaia M, et al. The opposite effects of IL-15 and IL-21 on CLL B cells correlate with differential activation of the JAK/STAT and ERK1/2 pathways. *Blood*. 2008;111(2):517-524.
21. Rentzos M, Cambouri C, Rombos A, et al. IL-15 is elevated in serum and cerebrospinal fluid of patients with multiple sclerosis. *J Neurol Sci*. 2006;241(1-2):25-29.
22. Lee YB, Satoh J, Walker DG, Kim SU. Interleukin-15 gene expression in human astrocytes and microglia in culture. *Neuroreport*. 1996;7(5):1062-1066.
23. Tagaya Y, Kurys G, Thies TA, et al. Generation of secretable and nonsecretable interleukin 15 isoforms through alternate usage of signal peptides. *Proc Natl Acad Sci U S A*. 1997;94(26):14444-14449.

584 24. Giri JG, Kumaki S, Ahdieh M, et al. Identification and cloning of a novel IL-
585 15 binding protein that is structurally related to the alpha chain of the IL-2 receptor.
586 *EMBO J*. 1995;14(15):3654-3663.
587 25. Bergamaschi C, Bear J, Rosati M, et al. Circulating IL-15 exists as
588 heterodimeric complex with soluble IL-15Ralpha in human and mouse serum. *Blood*.
589 2012;120(1):e1-8.
590 26. Diamanti P, Cox CV, Moppett JP, Blair A. Parthenolide eliminates leukemia-
591 initiating cell populations and improves survival in xenografts of childhood acute
592 lymphoblastic leukemia. *Blood*. 2013;121(8):1384-1393.
593 27. Cox CV, Diamanti P, Evely RS, Kearns PR, Blair A. Expression of CD133 on
594 leukemia-initiating cells in childhood ALL. *Blood*. 2009;113(14):3287-3296.
595 28. Halsey C, Docherty M, McNeill M, et al. The GATA1s isoform is normally
596 down-regulated during terminal haematopoietic differentiation and over-expression
597 leads to failure to repress MYB, CCND2 and SKI during erythroid differentiation of
598 K562 cells. *J Hematol Oncol*. 2012;5:45.
599 29. Cosimo E, McCaig AM, Carter-Brzezinski LJ, et al. Inhibition of NF-kappaB-
600 Mediated Signaling by the Cyclin-Dependent Kinase Inhibitor CR8 Overcomes
601 Prosurvival Stimuli to Induce Apoptosis in Chronic Lymphocytic Leukemia Cells.
602 *Clin Cancer Res*. 2013;19(9):2393-2405.
603 30. Tagaya Y, Bamford RN, DeFilippis AP, Waldmann TA. IL-15: a pleiotropic
604 cytokine with diverse receptor/signaling pathways whose expression is controlled at
605 multiple levels. *Immunity*. 1996;4(4):329-336.
606 31. Malamut G, El Machhour R, Montcuquet N, et al. IL-15 triggers an
607 antiapoptotic pathway in human intraepithelial lymphocytes that is a potential new
608 target in celiac disease-associated inflammation and lymphomagenesis. *J Clin Invest*.
609 2010;120(6):2131-2143.
610 32. Wilkinson PC, Liew FY. Chemoattraction of human blood T lymphocytes by
611 interleukin-15. *J Exp Med*. 1995;181(3):1255-1259.
612 33. McInnes IB, al-Mughales J, Field M, et al. The role of interleukin-15 in T-cell
613 migration and activation in rheumatoid arthritis. *Nat Med*. 1996;2(2):175-182.
614 34. Hart G, Avin-Wittenberg T, Shachar I. IL-15 regulates immature B-cell
615 homing in an Ly49D-, IL-12 , and IL-18 dependent manner. *Blood*. 2008;111(1):50-
616 59.
617 35. Lodolce JP, Boone DL, Chai S, et al. IL-15 receptor maintains lymphoid
618 homeostasis by supporting lymphocyte homing and proliferation. *Immunity*.
619 1998;9(5):669-676.
620 36. Kivisakk P, Mahad DJ, Callahan MK, et al. Human cerebrospinal fluid central
621 memory CD4+ T cells: evidence for trafficking through choroid plexus and meninges
622 via P-selectin. *Proc Natl Acad Sci U S A*. 2003;100(14):8389-8394.
623 37. Sorensen TL. Targeting the chemokine receptor CXCR3 and its ligand
624 CXCL10 in the central nervous system: potential therapy for inflammatory
625 demyelinating disease? *Curr Neurovasc Res*. 2004;1(2):183-190.
626 38. Huhmer AF, Biringer RG, Amato H, Fonteh AN, Harrington MG. Protein
627 analysis in human cerebrospinal fluid: Physiological aspects, current progress and
628 future challenges. *Dis Markers*. 2006;22(1-2):3-26.
629 39. Allavena P, Giardina G, Bianchi G, Mantovani A. IL-15 is chemotactic for
630 natural killer cells and stimulates their adhesion to vascular endothelium. *J Leukoc*
631 *Biol*. 1997;61(6):729-735.

40. Harakawa N, Shigeta A, Wato M, et al. P-selectin glycoprotein ligand-1 mediates L-selectin-independent leukocyte rolling in high endothelial venules of peripheral lymph nodes. *Int Immunol*. 2007;19(3):321-329.
41. Balashov KE, Rottman JB, Weiner HL, Hancock WW. CCR5(+) and CXCR3(+) T cells are increased in multiple sclerosis and their ligands MIP-1alpha and IP-10 are expressed in demyelinating brain lesions. *Proc Natl Acad Sci U S A*. 1999;96(12):6873-6878.
42. Kwaan HC, Wang J, Svoboda K, Declerck PJ. Plasminogen activator inhibitor 1 may promote tumour growth through inhibition of apoptosis. *Br J Cancer*. 2000;82(10):1702-1708.
43. Bajou K, Noel A, Gerard RD, et al. Absence of host plasminogen activator inhibitor 1 prevents cancer invasion and vascularization. *Nat Med*. 1998;4(8):923-928.
44. Klein RM, Bernstein D, Higgins SP, Higgins CE, Higgins PJ. SERPINE1 expression discriminates site-specific metastasis in human melanoma. *Exp Dermatol*. 2012;21(7):551-554.
45. Samarakoon R, Higgins PJ. Pp60c-src mediates ERK activation/nuclear localization and PAI-1 gene expression in response to cellular deformation. *J Cell Physiol*. 2003;195(3):411-420.
46. Case M, Matheson E, Minto L, et al. Mutation of genes affecting the RAS pathway is common in childhood acute lymphoblastic leukemia. *Cancer Res*. 2008;68(16):6803-6809.
47. Hoelbl A, Schuster C, Kovacic B, et al. Stat5 is indispensable for the maintenance of bcr/abl-positive leukaemia. *EMBO Mol Med*. 2010;2(3):98-110.
48. Roberts KG, Morin RD, Zhang J, et al. Genetic alterations activating kinase and cytokine receptor signaling in high-risk acute lymphoblastic leukemia. *Cancer Cell*. 2012;22(2):153-166.
49. Klebanoff CA, Finkelstein SE, Surman DR, et al. IL-15 enhances the in vivo antitumor activity of tumor-reactive CD8+ T cells. *Proc Natl Acad Sci U S A*. 2004;101(7):1969-1974.
50. Bondurant KL, Lundgreen A, Herrick JS, Kadlubar S, Wolff RK, Slattery ML. Interleukin genes and associations with colon and rectal cancer risk and overall survival. *International Journal of Cancer*. 2013;132(4):905-915.

FIGURE LEGENDS

Figure 1:

IL-15 and IL-15 receptor expression by pre-B ALL cells and correlation with CNS infiltration. (A) RT-PCR analysis of IL-15 isoform and IL-15 receptor expression by cell lines and primary patient samples. Expected sizes in brackets; LSP-IL-15 (201bp), SSP-IL-15 (320bp), IL-15Rα (402bp), IL-15/2Rβ (403bp), IL-15/2Rγ (447bp), GAPDH (Housekeeping control) (115bp). Representative examples are shown; individual results are listed in supplementary table 1. (B) SYBR green relative quantification of IL-15 mRNA expression in primary patient samples using SD-1 as the calibrator

(expression in patient samples reported as fold change relative to the level of expression in SD-1 cells, arbitrarily set at 1). (C) Histological analysis of murine brains and spinal cord from xenografts. Top panel left to right: SD-1, Sup-B15 and REH H&E stained sections showing dark purple leukaemic cells infiltrating the meninges (thick arrows) (all x10 magnification, black scale bars represent 100µm). Bottom panel immunohistochemistry for human CD45 confirms the human origin of these infiltrating cells (isotype control shown in small inset panel) (x40 magnification, black scale bars represent 100µm). Bottom right panel, section through spinal cord from SD-1 xenograft; stars mark the sites of leukaemic infiltration in the meningeal covering of the spinal cord (x20 magnification, black scale bars represent 100µm). (D) Time to hind-limb paralysis of cell line xenografts, 4-8 mice per cell line. (E-H) Taqman qPCR analysis of IL-15 and all three components of the IL-15 receptor complex in xenografted cell lines. Three independent cultures were analysed per cell line, all results are expressed relative to the level in Sup-B15 cells, arbitrarily set at 1.0. All data are mean ± S.E.M and were analysed by student t-tests comparing SD-1 cells to each of the other cell lines . ***$p<0.001$, **$p<0.01$, *$p<0.05$, n.s = not significant.

Figure 2

Pre-B ALL primary cells and SD-1 cells show increased growth in the presence of IL-15. (A) Six different primary pre-B ALL samples were grown in optimised 3-cytokine mix with or without addition of IL-15 (25ng/ml). Numbers of viable blast cells were measured at weeks 1, 2 and 3 by flow cytometry. Each sample is shown individually and then results from all 6 experiments are pooled (bottom panel, data represent mean ± S.E.M) (B) Fold change in cell numbers compared to baseline (starting cell count at initiation of the experiment) was calculated for the two experimental conditions in each of the 6 primary samples. Data were analysed using a Wilcoxon matched-pairs sign rank test, bars display mean ± S.E.M. (C) Growth of SD-1, Sup-B15, REH and SEM cells following treatment with 1, 5 or 25 ng/ml IL-15 for up to 96 h. (D) Growth of SD-1 and SupB-15 cells following treatment with media alone, 6

μg/ml isotype control antibody or 6 μg/ml of IL-15Rα nAb. Viable cells were determined using trypan blue. Data represent mean ± S.E.M. Data were analysed using an unpaired student t test. *p<0.05 and are representative of 3 independent experiments carried out per cell line.

Figure 3:

IL-15 has no effect on apoptosis in SD-1 cells. (A) Intracellular IL-15 protein levels in SD-1 and Sup-B15 cells, measured by flow cytometry with isotype (shaded) and IL-15 specific Ab (open). Corrected mean fluorescence intensity (MFI) represents MFI IL-15PE – MFI isotype control. (B) Levels of IL-15Rα, β and γ in SD-1 and Sup-B15 cells, determined by western blot with β-tubulin as a loading control. MOLT-4 cells expressing high levels of IL-15Rα were used as a positive control (C) Western blot for BCL-xL and BCL-2 protein expression in SD-1 cells treated with IL-15 (1, 5 and 25 ng/ml) for 72 h. (D) PARP cleavage in SD-1 cells treated with IL-15 (25 ng/ml) for 96 h. The positive control lane contains SD-1 cells treated with the apoptosis-inducing agent AA2 (50 μM) for 1 h. Histone H3 was used as loading control. (E) Annexin V-FITC and PI staining of SD-1 cells treated with (right panel) or without (central panel) 25 ng/ml IL-15 for 96h. The positive control shows cells exposed to AA2 (50 μM) for 1 h (left panel). (F) SD-1 cells (dark bars) and the dexamethasone sensitive cell line CCRF-CEM (light bars; used as a positive control) were exposed to vehicle (0.1% EtOH) or dexamethasone (100 nM, 1 μM or 10 μM) for 48h. Percentage apoptosis (sum of early and late apoptosis) of these cells was then measured using an Annexin V assay. Data represent mean ± S.E.M with n=3 for each cell line. (G) SD-1 (dark bars) and CCRF-CEM cells (light bars) were exposed to similar conditions as (C) for 48 h and viability was assessed using an MTT assay. Data show viability (% of control) compared to untreated control. (H) MTT assay of SD-1 (dark bars) and CCRF-CEM (light bars) cells exposed to dexamethasone (10μM) ± IL-15Rα nAb/isotype control for 72 h. In (F) – (H), data represent mean +/- SEM (n=3) and were analysed using a Kruskal Wallis test with Dunn's multiple

comparison test. **p<0.01, ***p<0.001.

Figure 4:

IL-15 promotes growth of SD-1 cells under low serum conditions, which is independent of apoptosis. (A) SD-1 cells were grown in RPMI media without addition of FCS, with (dashed line) or without (solid line) 25ng/ml of IL-15. The growth curve from one representative experiment of 3 is shown (B) SD-1 cells were grown in RPMI supplemented with increasing concentrations of FCS with (black bars) or without (white bars) 25ng/ml of IL-15. The total number of viable cells in each group at 72 hours is shown. Data represent mean ± SEM from 3 independent experiments. Data were analysed by a Mann-Whitney test. *p<0.05, **p<0.01, ***p<0.001. (C) Percentage increase in cell counts of IL-15 treated SD-1 (dark bars) and Sup-B15 (light bars) compared to media control. Data represent mean ± SEM from 3 independent experiments. SD-1 data is from the same experiments as in (B) above represented in a different format. (D) PARP cleavage analysis of SD-1 cells exposed to increasing concentrations of serum ± 25ng/ml IL-15 for 96 h. The positive control lane represents SD-1 cells exposed to the apoptosis-inducing agent AA2 (50 μM) for 1 h. Histone H3 was used as a loading control.

Figure 5:

IL-15 is not directly chemotactic but induces expression of molecules associated with leukocyte trafficking. (A) SD-1 cells were placed in the top section of a bare filter transwell (5 μM pore size) and exposed to IL-15 (1, 10, 100, 300 or 1000 ng/ml) in the bottom section of the transwell. Transmigration was assessed following a 3 h incubation period. Migration index was calculated by counting the total number of cells transmigrated cells in response to IL-15 as a proportion of the total number of cells that transmigrated in response to chemotaxis buffer alone (spontaneous migration). Data shown are from one experiment performed in triplicate. (B) SD-1 cells (n=3 independent cultures) were treated with IL-15 (25 ng/ml) for 72 h and levels of mRNA encoding PSGL-1 and CXCR3 measured by qPCR. Results are expressed as relative quantities with the level in media alone

arbitrarily set to 1.0. (C) SD-1 cells (n=3 independent cultures) were treated as in (B) and the surface expression of PSGL-1 and CXCR3 was analysed by FACS. Corrected mean fluorescence intensity (cMFI) represents MFI specific antibody – MFI isotype control. (D) Following IL-15 treatment as in (B) above, expression of 95 genes associated with tumour metastasis was assessed using a commercially available RT^2 PCR profiler array. Data are represented as a scatter plot (RQ log10) and solid lines represent 2 fold down- or up-regulation. The 7 genes showing >2 fold change with IL-15 treatment are listed. (E) Validation of hits from (D) by qPCR of SD-1 cells (n=3 independent cultures) treated with media ± IL-15 (25 ng/ml) for 72 h confirmed modest up-regulation of Serpine1 by IL-15. Data show the number of copies of Serpine 1 per 1000 copies of the housekeeping control gene TBP. All data are mean ± S.E.M and were analysed by unpaired student t-tests. *p<0.05, **p<0.01, ***p<0.001.

Figure 6:

STAT5 and ERK1/2 signalling pathways are activated by IL-15 in SD-1 cells. (A) SD-1 cells were treated with IL-15 (25 ng/ml) for 15, 30, 45, 60 or 120 min. Cell lysates were analysed by western blot using antibodies as indicated. (B) Western blot band density was analysed via ImageJ software (NIH) and adjusted densitometry values for p-STAT5 calculated by dividing the relative densities for p-STAT5 by the relative densities for total STAT5. (C) Adjusted densities values for p-ERK1/2 and (D) p-IκBα were calculated in a manner similar to above, except that relative densities for total ERK1/2 and IκBα were used respectively.

Figure 7:

IL-15-induced proliferation of SD-1 cells is mediated via the MEK/ERK signalling pathway. SD-1 cells were treated with (A) 10 μM ERK1/2 inhibitor (dashed lines), (B) 100 μM STAT5 inhibitor (dashed lines), (C) 10 μM MEK inhibitor (dashed lines), (D) 5μM NFκB inhibitor (IKK-2 inhibitor IV) or 20μM PI3K inhibitor (LY 294002) or matched vehicle controls (0.1% DMSO) (solid

lines) with (solid symbols) or without (open symbols) additional IL-15 (25ng/ml). Viable cell numbers were determined using trypan blue. Data are mean ± S.E.M. Unpaired student t-tests were used to compare cell counts at 72 and 96h in drug treated IL-15 *vs.* no IL-15 groups. *p<0.05, **p<0.01, n.s = no significant difference. Vehicle treated IL-15 *vs.* no IL-15 groups showed significant (p<0.05) increase in cell numbers with IL-15 treatment at 72 and 96h as previously shown (figure 2c). Representative graphs of 3 independent experiments are shown.

Figure 1

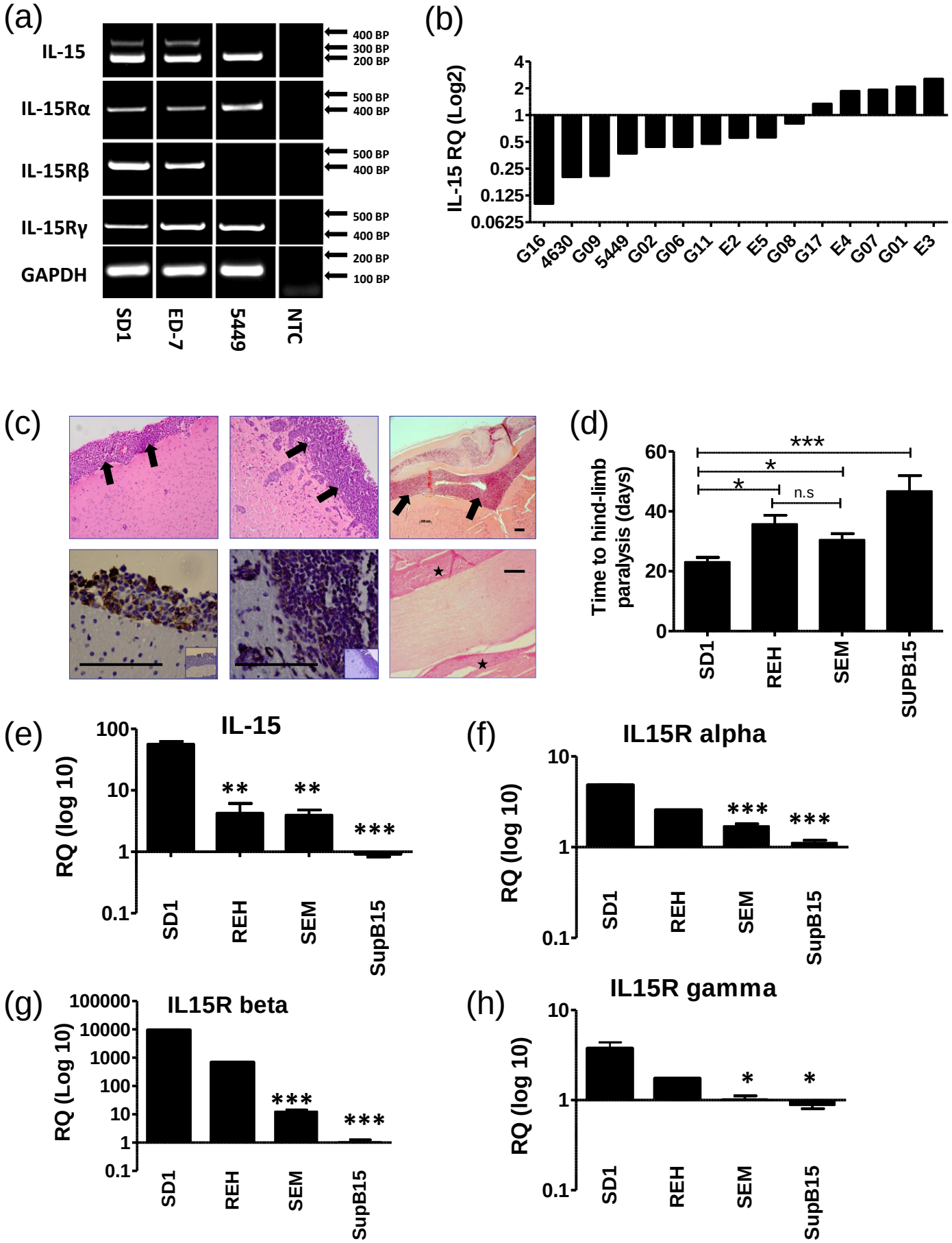
(a)
IL-15
IL-15Rα
IL-15Rβ
IL-15Rγ
GAPDH
400 BP
300 BP
200 BP
500 BP
400 BP
500 BP
400 BP
500 BP
400 BP
200 BP
100 BP
SD1
ED-7
5449
NTC
(b)
IL-15 RQ (Log2)
4
2
1
0.5
0.25
0.125
0.0625
G16
4630
G09
5449
G02
G06
G11
E2
E5
G08
G17
E4
G07
G01
E3
(c)
(d)
Time to hind-limb paralysis (days)
60
40
20
0
***
*
*
n.s
SD1
REH
SEM
SUPB15
(e)
IL-15
RQ (log 10)
100
10
1
0.1
**
**
***
SD1
REH
SEM
SupB15
(f)
IL15R alpha
RQ (log 10)
10
1
0.1
***
***
SD1
REH
SEM
SupB15
(g)
IL15R beta
RQ (Log 10)
100000
10000
1000
100
10
1
0.1
***
***
SD1
REH
SEM
SupB15
(h)
IL15R gamma
RQ (log 10)
10
1
0.1
*
*
SD1
REH
SEM
SupB15

Figure 2 New figure

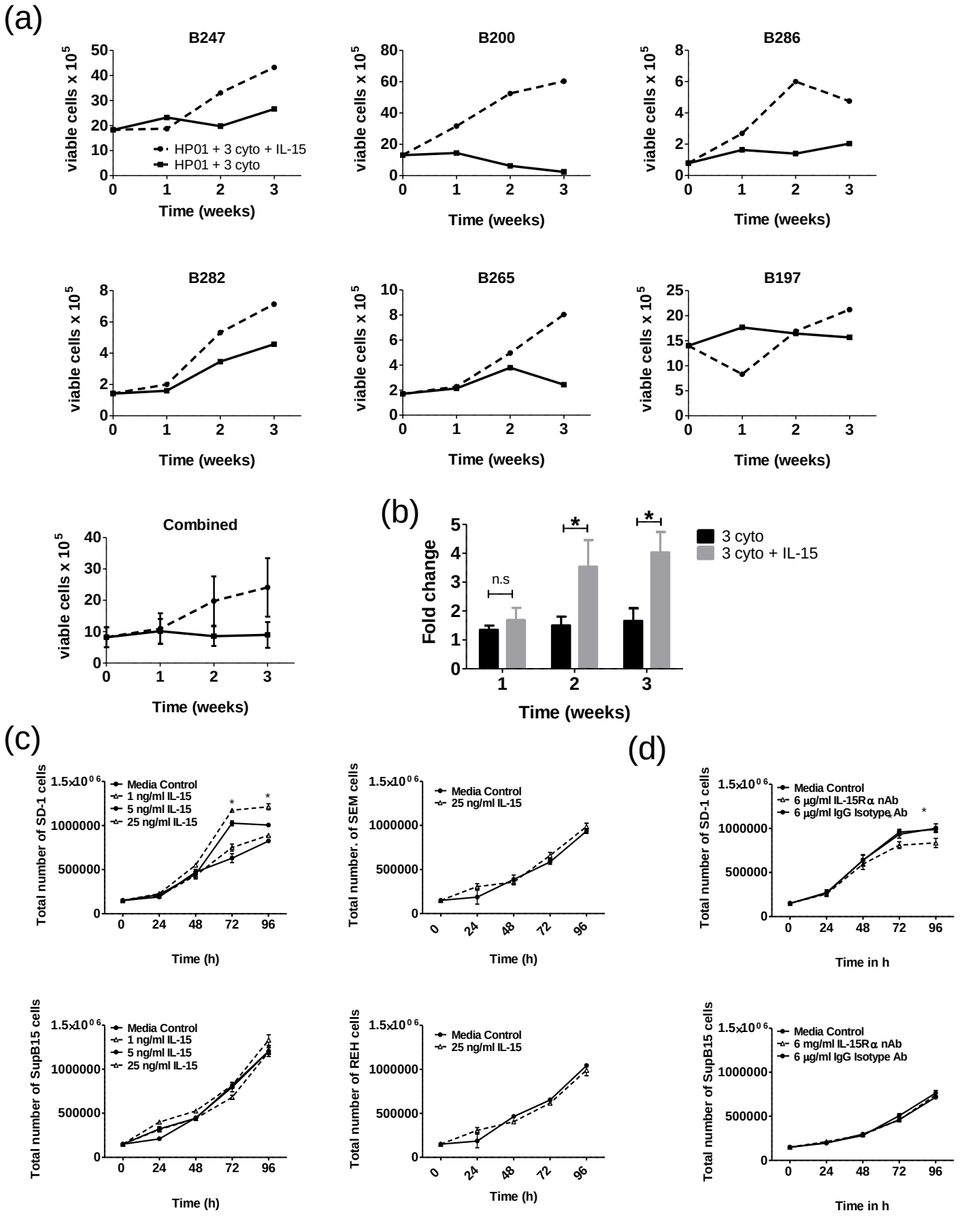

Figure 3

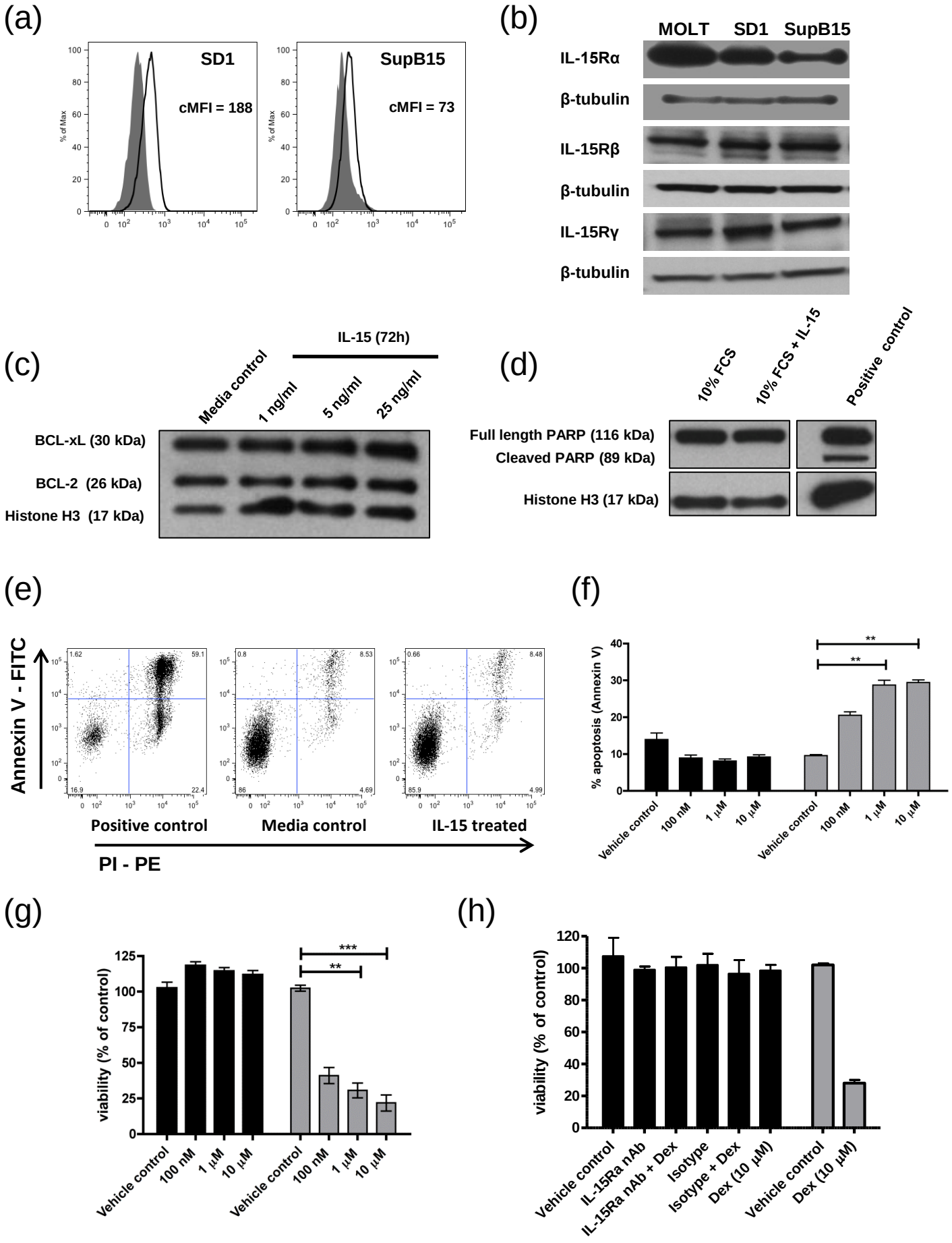
(a)
SD1
cMFI = 188
SupB15
cMFI = 73
% of Max
(b)
MOLT
SD1
SupB15
IL-15Rα
β-tubulin
IL-15Rβ
β-tubulin
IL-15Rγ
β-tubulin
(c)
IL-15 (72h)
Media control
1 ng/ml
5 ng/ml
25 ng/ml
BCL-xL (30 kDa)
BCL-2 (26 kDa)
Histone H3 (17 kDa)
(d)
10% FCS
10% FCS + IL-15
Positive control
Full length PARP (116 kDa)
Cleaved PARP (89 kDa)
Histone H3 (17 kDa)
(e)
Annexin V - FITC
PI - PE
Positive control
Media control
IL-15 treated
(f)
% apoptosis (Annexin V)
Vehicle control
100 nM
1 μM
10 μM
(g)
viability (% of control)
(h)
viability (% of control)
Vehicle control
IL-15Ra nAb
IL-15Ra nAb + Dex
Isotype
Isotype + Dex
Dex (10 μM)

Figure 4

(a)

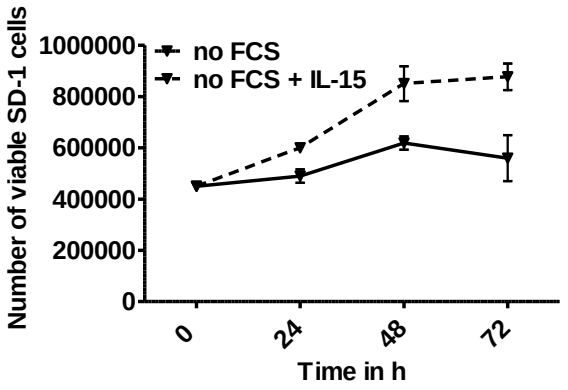

(b)

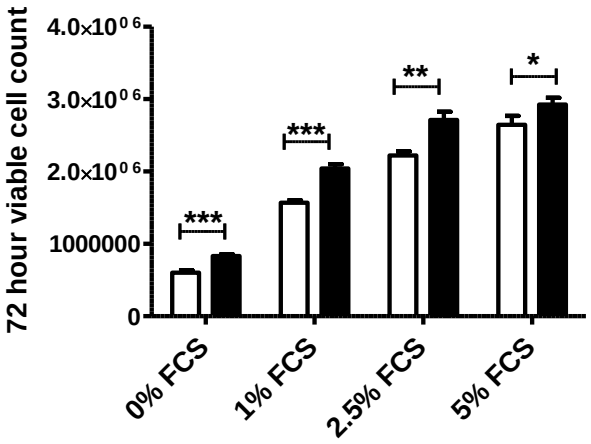

(c)

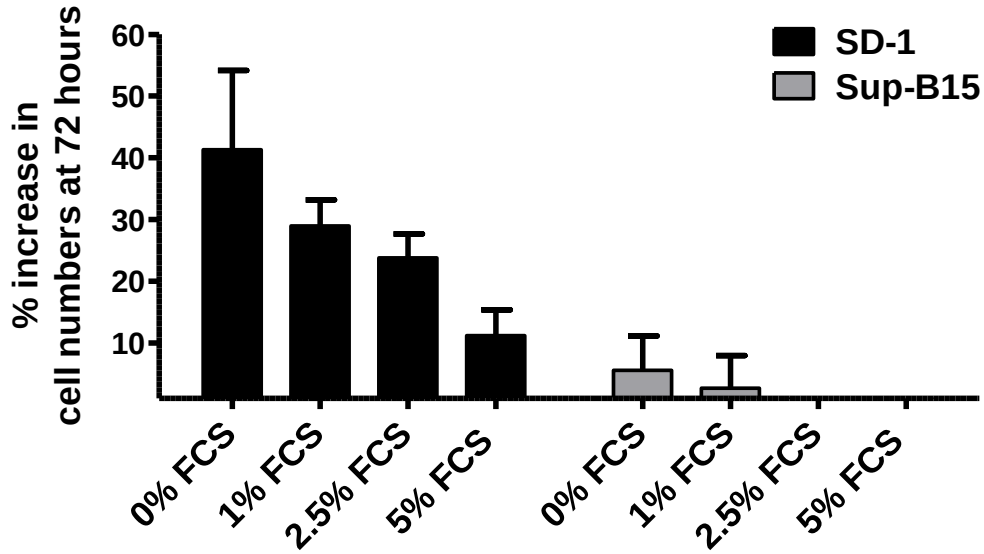

(d)

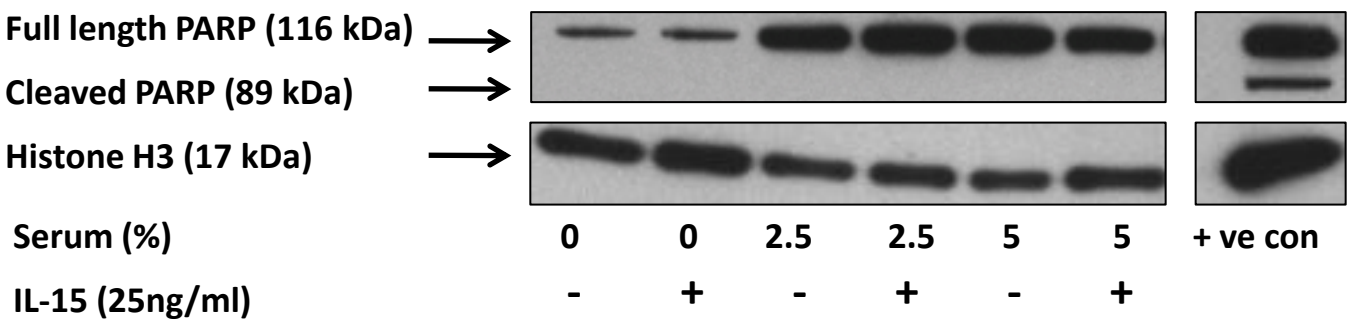

Figure 5

(a)

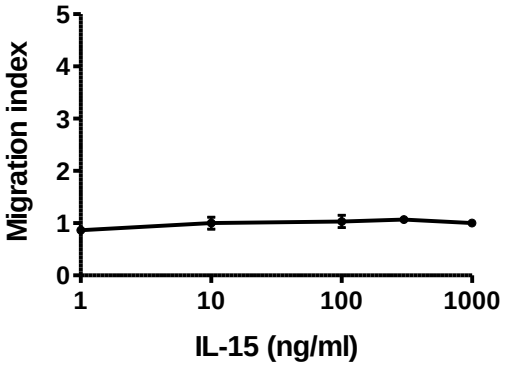

(b)

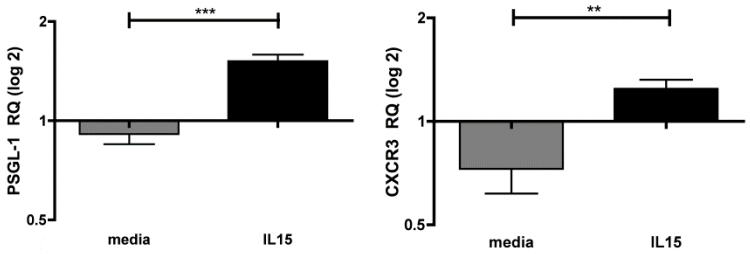

(c)

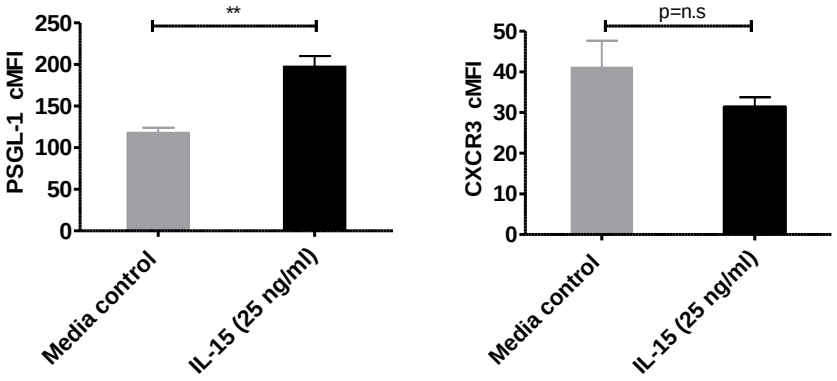

(d)

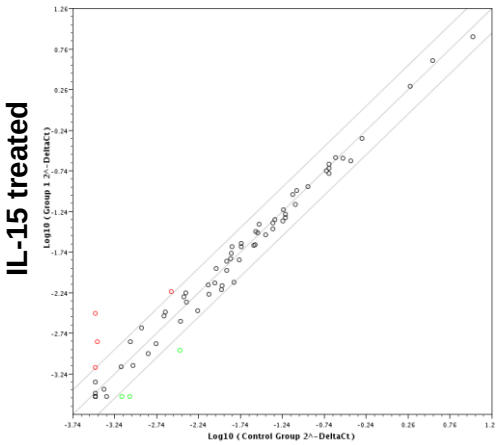

Gene	Fold change
CDH11	4.0058
MMP9	2.0327
PTEN	2.176
SERPINE1	9.5507
DENR	-3.0873
MMP3	-2.3077
TIMP4	-2.8562

(e)

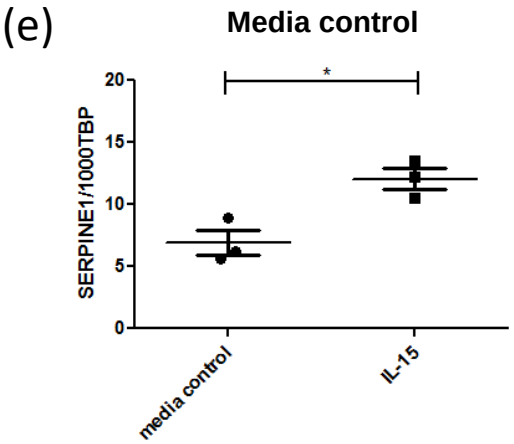

Figure 6

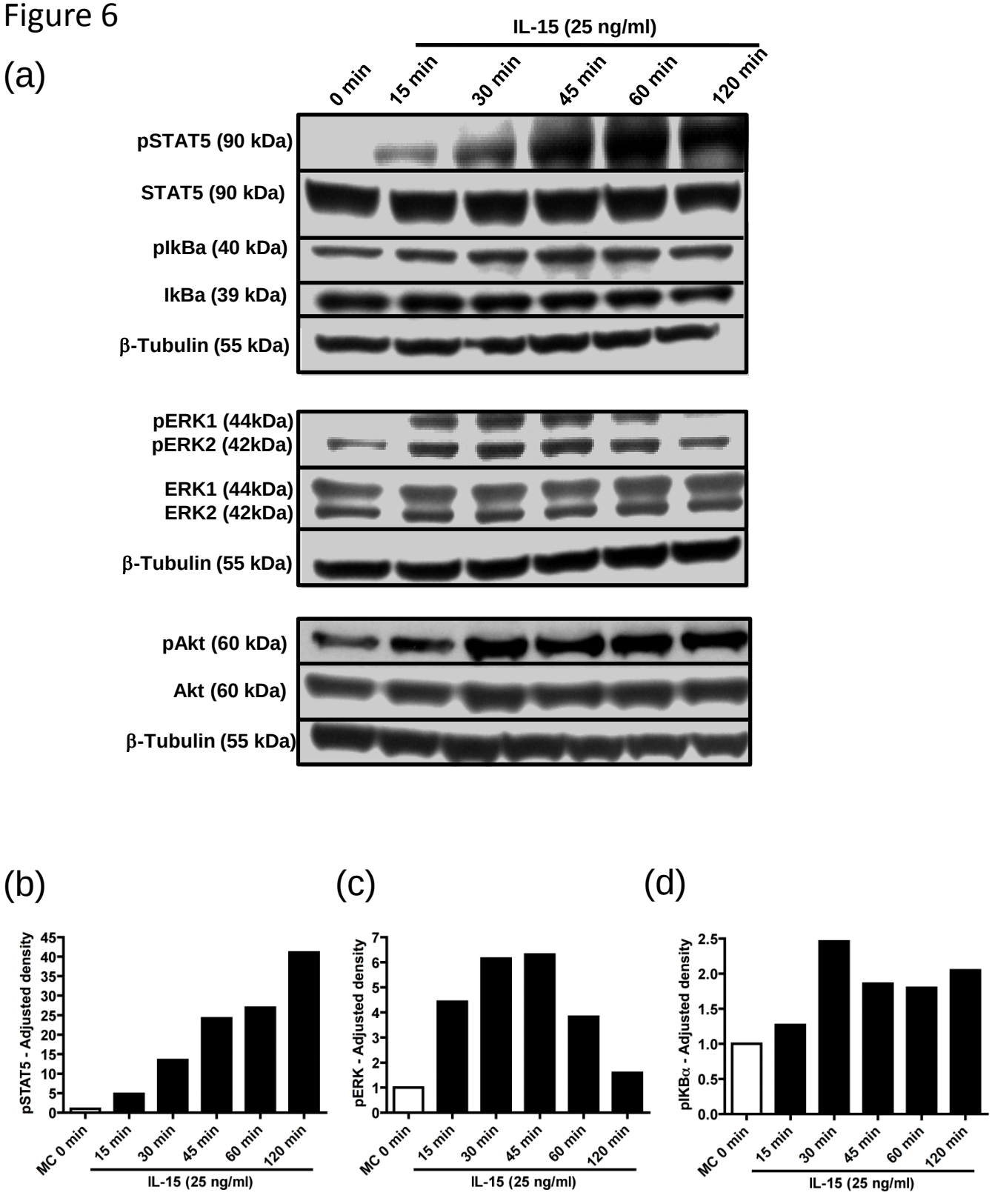
(a)
IL-15 (25 ng/ml)
0 min
15 min
30 min
45 min
60 min
120 min
pSTAT5 (90 kDa)
STAT5 (90 kDa)
pIkBa (40 kDa)
IkBa (39 kDa)
β-Tubulin (55 kDa)
pERK1 (44kDa)
pERK2 (42kDa)
ERK1 (44kDa)
ERK2 (42kDa)
β-Tubulin (55 kDa)
pAkt (60 kDa)
Akt (60 kDa)
β-Tubulin (55 kDa)
(b)
pSTAT5 - Adjusted density
MC 0 min
15 min
30 min
45 min
60 min
120 min
IL-15 (25 ng/ml)
(c)
pERK - Adjusted density
MC 0 min
15 min
30 min
45 min
60 min
120 min
IL-15 (25 ng/ml)
(d)
pIKBα - Adjusted density
MC 0 min
15 min
30 min
45 min
60 min
120 min
IL-15 (25 ng/ml)

Figure 7

(a)

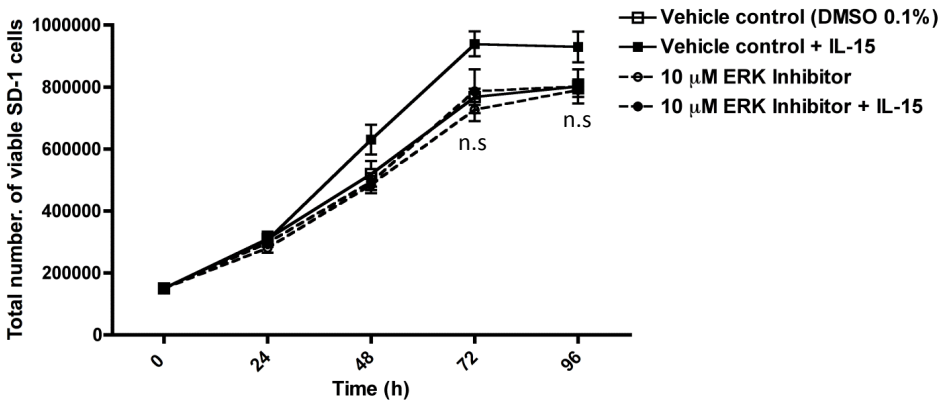

(b)

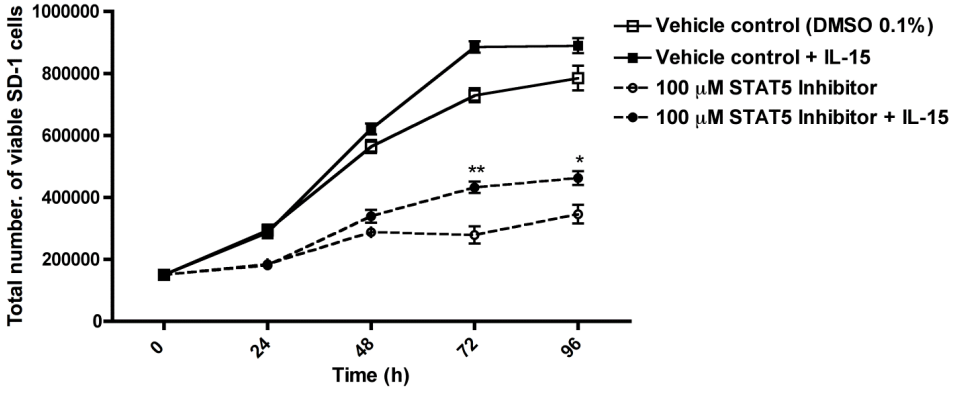

(c)

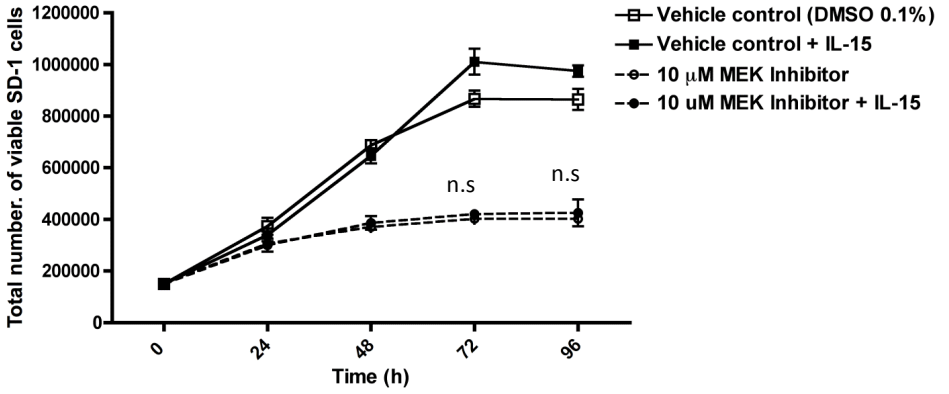

(d)

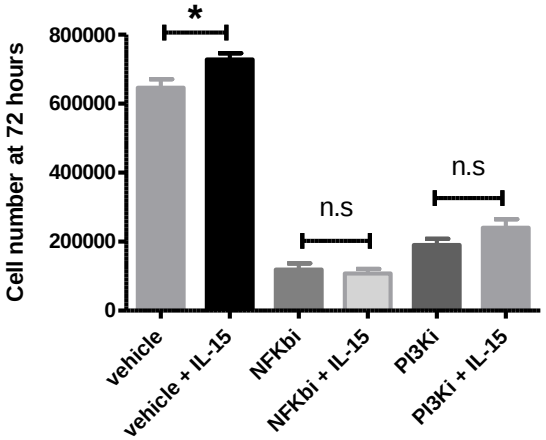

Supplementary Data

ALL patient and cell line details													
ID	**Sex**	**Age (Years)**	**WCC ($x10^9$/l)**	**Cytogenetics**	**Immunophenotype**	**CNS status**	**Outcome**	**IL15 RQ**	**IL15 LSP**	**IL15 SSP**	**IL15 Rα**	**IL15 Rβ**	**IL15 Rγ**
Cell lines													
SD1	F	n/k	n/k	t(9;22)	CD34+, CD10neg, CD19+, Cyt79a+	n/k	n/k	1	Y	Y	Y	Y	Y
Sup B15	M	8	n/k	t(9;22)	CD10+, sIg neg	n/k	n/k	0.082	Y	Y	Y	Y	Y
REH	F	15	n/k	t(12;21)	CD34neg, CD10+, CD19+, Cyt79a+	n/k	Established at time of 1st relapse	0.384	Y	Y	Y	Y	Y
SEM	F	5	n/k	t(4:11)	CD34neg, CD19+,	n/k	Established at time of 1st relapse	0.337	Y	N	Y	Y	Y
Patients													
G01	M	2	23	11q23	CD34+, TdTneg, CD10+, CD19+, Cyt79a+	1	CCR (19 months)	2.09	Y	Y	Y	Y	Y
G02	F	5	29	t(12;21)	CD34lo, TdT+, CD10+, CD19+, Cyt79a+	1	CCR (19 months)	0.44	Y	N	Y	Y	Y
G06	M	4	52	t(12;21)	CD34+, TdT+, CD10+, CD19+, Cyt79a+	1	CCR (13 months)	0.44	Y	Y	Y	Y	Y
G07	M	10	3	Normal	CD34+, TdT+, CD10+, CD19+, Cyt79a+	1	CCR (13 months)	1.93	Y	Y	Y	Y	Y
G08	F	11	35	dic(7;9)	CD34+, TdT+, CD10lo, CD19+, Cyt79a+	1	CCR (13 months)	0.80	Y	N	Y	Y	Y
G09	F	6	23	Hyperdiploid	CD34+, TdT+, CD10+, CD19+, Cyt79a+	1	CCR (13 months)	0.21	Y	Y	Y	Y	Y
G11	M	10	14	High Hyperdiploid	CD34+, TdT+, CD10+, CD19+, Cyt79a+	TLP+	CCR (11 months)	0.48	Y	N	Y	Y	Y
G16	M	2	90	High Hyperdiploid	CD34+, TdT+, CD10+, CD19+, Cyt79a+	1	CCR (10 months)	0.10	Y	N	Y	Y	Y
G17	F	3	50	t(12;21)	CD34+, TdT+, CD10+, CD19+, Cyt79a+	1	CCR (9 months)	1.34	Y	Y	Y	Y	Y
E2	F	3	34.4	Hyperdiploid	CD34+, TdT+, CD10+, Cyt79a+	1	CCR (21 months)	0.56	Y	N	Y	Y	Y

E3	F	6	9.6	t(12;21)	CD34+, TdT+, CD10+, Cyt79a+	1	CCR (21 months)	2.56	Y	N	Y	Y	Y
E4	M	3	16.8	Hyperdiploid	CD34+, TdT+, CD10+, CD20+, Cyt79a+	1	CCR (20 months)	1.86	Y	N	Y	Y	Y
E5	F	2	4.3	t(12;21)	CD34lo, TdT+, CD10+, Cyt79a+	1	Died during induction* (week 3)	0.56	Y	N	Y	Y	Y
5449	F	2.5	62.2	t(12;21)	B-precursor	1	CCR (5.3 years)	0.37	Y	N	Y	N	Y
4630	F	2.9	103.6	t(12;21)	B-precursor	1	CCR (7.0 years)	0.20	Y	N	Y	N	Y
5094	F	2.1	84.6	t(12;21)	B-precursor	3	CCR (6.6 years)	n.d	Y	N	Y	N	Y
4736	F	3.5	113.3	t(12;21)	B-precursor	1	CCR (6.1 years)	n.d	Y	Y	Y	Y	Y
5705	F	3.4	221	t(12;21)	B-precursor	1	CCR (4.7 years)	n.d	Y	N	n.d	n.d	n.d
6294	F	1.8	24.5	High Hyperdiploid	B-precursor	1	CCR (3.0 years)	n.d	Y	N	n.d	n.d	Y
B200	F	2.9	n/k	t(12;21)	CD34+, TdT+, CD10+, CD19+, Cyt79a+	n/k	Relapsed (20 months)	n.d	n.d	n.d	n.d	n.d	n.d
B247	M	2	n/k	t(12;21)	CD34+, TdT+, CD10+, CD19+, Cyt79a+	n/k	CCR (2.7 years)	n.d	n.d	n.d	n.d	n.d	n.d
B265	F	5.9	n/k	t(12;21)	CD34+, TdT+, CD10+, CD19+	n/k	CCR (10 months)	n.d	n.d	n.d	n.d	n.d	n.d
B197	M	4	n/k	t(1:19)	CD34neg, TdT+, CD10+, CD19+, Cyt79a+	n/k	CCR (4.25 years)	n.d	n.d	n.d	n.d	n.d	n.d
B286	M	4.5	n/k	High Hyperdiploid	B-precursor	n/k	CCR (9 months)	n.d	n.d	n.d	n.d	n.d	n.d
B282	F	0.66	n/k	Hyperdiploid	B-precursor	n/k	Consolidation therapy (3 months)	n.d	n.d	n.d	n.d	n.d	n.d

Table S1: Patient and cell line details and results of IL-15 and IL-15 receptor RT-PCR and IL-15 qPCR. n.d = not done due to lack of material. CCR=continuous complete remission. n/k = not known. CNS-1 (CSF white cell count (WCC) <5/µl, no blasts), CNS-2 (WCC<5/µl, visible blasts) or CNS-3 (WCC>5/µl), TLP+ = traumatic lumbar puncture with visible blasts. *= death due to haemorrhage.

RT-PCR			
Target	Sequence	Annealing temperature	Product size
IL-15	5′ AAA CCC CTT GCC ATA GCC AGC TCT T 3′ CTT CTG TTT TAG GAA GCC CTG CAC T	55°C	201bp LSP-IL-15 320bp SSP-IL-15
IL-15Rα	5′ GCC AGC GCC ACC CTC CAC AGT AA 3′ GCC AGC GGG GGA GTT TGC CTT GAC	55°C	402bp
IL-15Rβ	5′ CAC AGA TGC AAC ATA AGC TGG 3′ ACT TCA GGA CCT TCT TCA GCC	52°C	403bp
IL-15Rγ	5′ AGC CCC AGC CTA CCA ACC TCA CT 3′ TTA AAG CGG CTC CGA ACA CGA A	55°C	447bp
Serpine 1	5′ GGTTCTGCCCAAGTTCTCC 3′ CGGTCATTCCCAGGTTCTC	60°C	71bp
GAPDH*	5′ CAAGGCTGAGAACGGGAA 3′ GGTGGTGAAGACGCCAGT	55°C	115bp

Taqman primers/probes			
Gene	Assay ID	Gene	Assay ID
GAPDH *	Hs99999905_m1	CX3CR1	Hs00365842_m1
IL-15	Hs99999039_m1	CXCR7	Hs00604567_m1
IL-15Ralpha	Hs00542604_m1	CXCR6	Hs00174843_m1
IL-15/2Rbeta	Hs01081697_m1	CXCR5	Hs00173527_m1
IL-15/2Rgamma	Hs00173950_m1	CXCR2	Hs00174304_m1
TBP*	Hs00427620_m1	CXCR1	Hs00174146_m1
ICAM3	Hs00233674_m1	CCR10	Hs00706455_s1
ICAM2	Hs00168384_m1	CCR8	Hs00174764_m1
ICAM1	Hs99999152_m1	CCR6	Hs00171121_m1
ITGB7	Hs00168469_m1	CCR4	Hs99999919_m1
ITGB2	Hs00164957_m1	CCR3	Hs00266213_s1
ITGB1	Hs01127543_m1	CCR1	Hs00174298_m1
ITGA4	Hs00168433_m1	SELPLG	Hs00380945_m1
ITGAL	Hs00158238_m1	CCR2	Hs00174150_m1
ITGAM	Hs00355885_m1	CCR5	Hs00152917_m1
NCAM1	Hs00941821_m1	CXCR3	Hs00171041_m1
SELL	Hs01046459_m1	CCR7	Hs01013469_m1
18sRNA*	Hs99999901_s1	CXCR4	Hs00237052_m1

Table S2: Primer/probe details for quantitative PCR. All Taqman probes were FAM-MGB labelled and were obtained from Applied Biosystems. *Endogenous control genes.

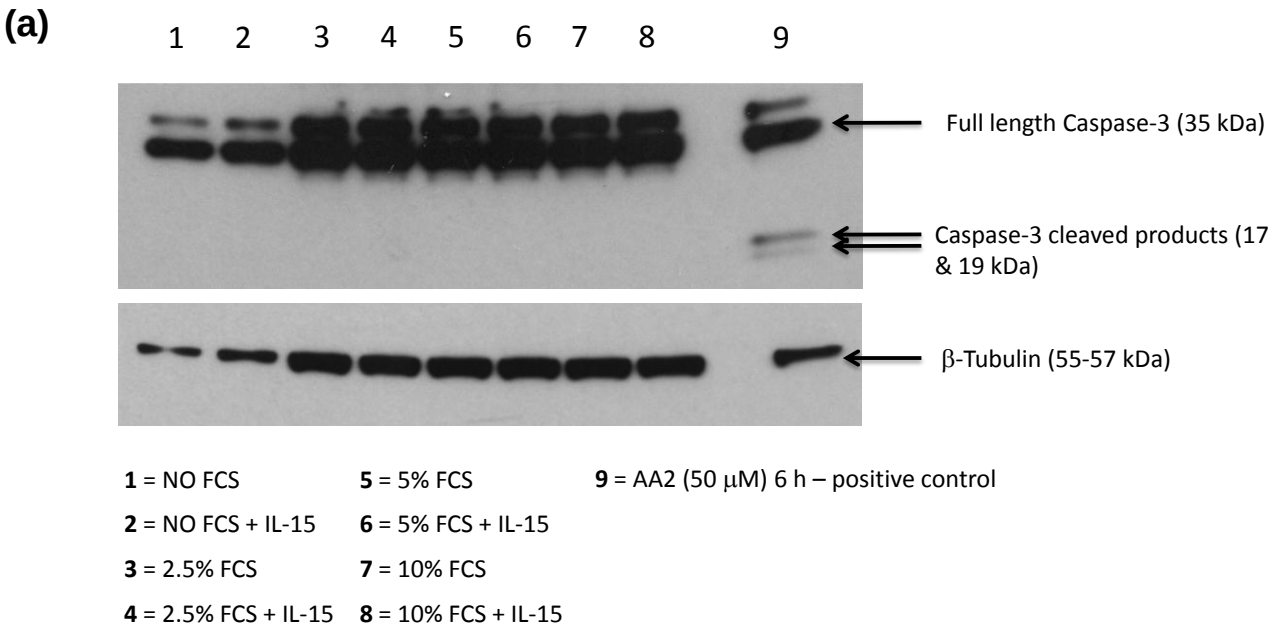

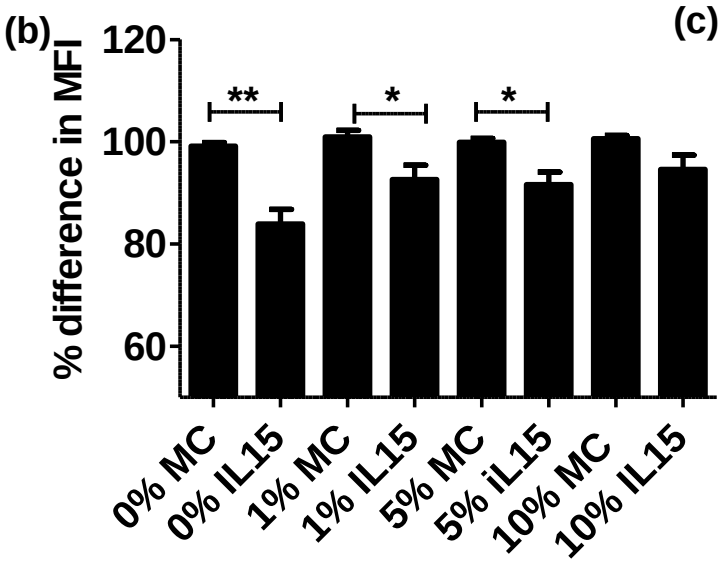

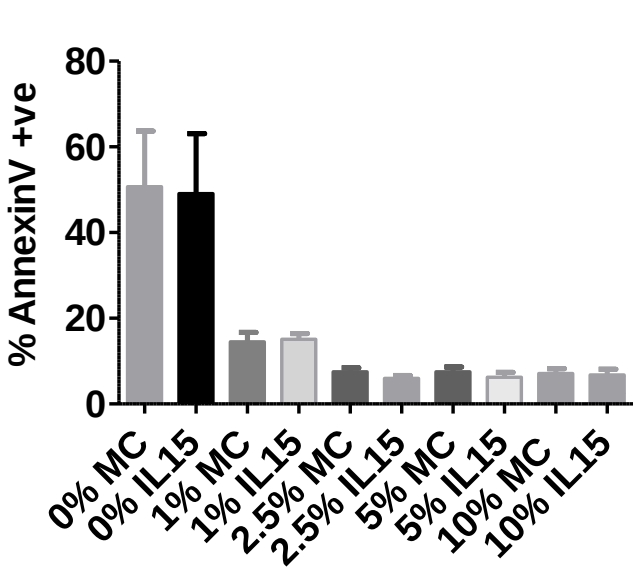

Figure S1: Effect of IL-15 on apoptosis and cell division in SD-1 cells grown under low serum conditions and in the absence and presence of IL-15. (a) SD-1 cells were exposed to differing concentrations of serum (0-10%) ± IL-15 (25 ng/ml) for 96 h. Whole cell lysates were created and then analysed for caspase-3 cleavage. The positive control lane represents SD-1 cells exposed to apoptosis activator compound 2 (AA2) (50 mM) for 1 hour. β-tubulin is shown as a loading control. (b) CellTrace Violet was used to analyse the number of cell divisions in IL-15 treated vs. untreated cells under normal and low serum conditions. Results are expressed as the percentage reduction in mean fluorescence intensity in IL-15 treated versus untreated cells measured after 72 hours incubation *p≤0.05, **p≤0.0.1. (c) As in (a) but using AnnexinV as a measure of apoptosis.

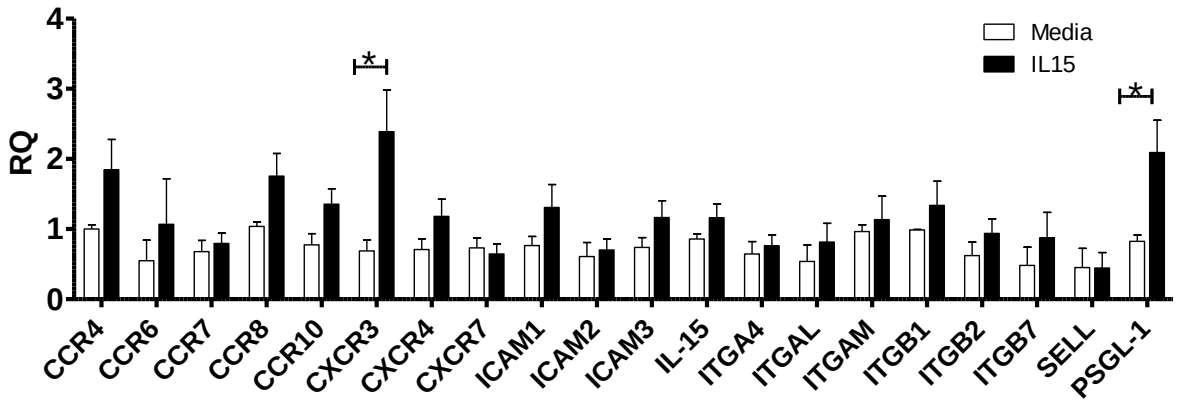

* The following genes had no detectable transcripts by qPCR: CCR1, CCR2, CCR3, CCR5, CXCR1, CXCR2, CXCR5, CXCR6, CX3CR1, NCAM.

Figure S2: Quantitative PCR for selectins, integrins and chemokine receptors in SD1 cells grown for 72 hours in media alone or media plus 25ng/ml IL-15. All data are shown as mean ± S.E.M and were analysed by a student t-test., *p≤0.05.

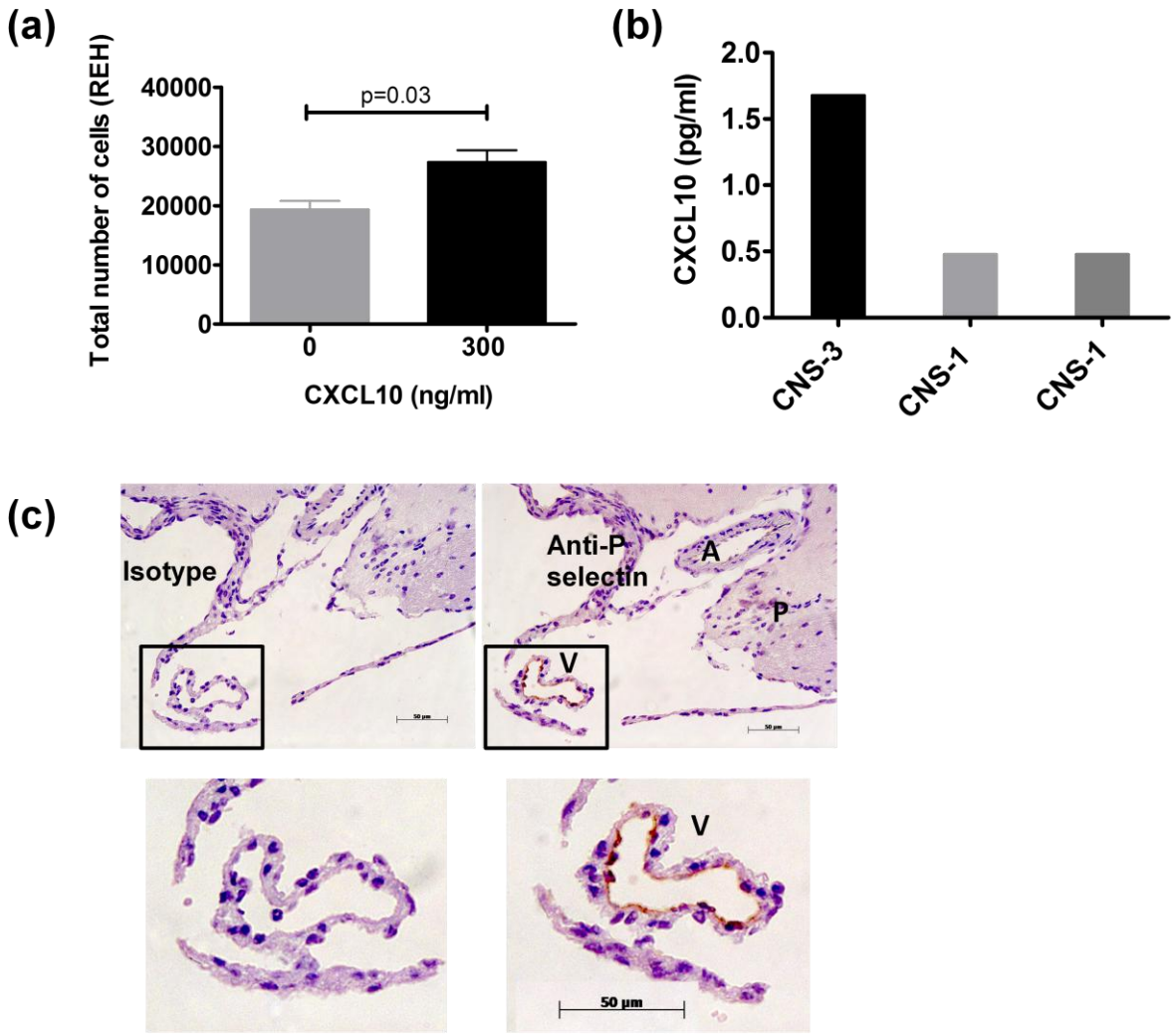

Figure S3: CXCR3 and PSGL-1 functional assessment. (a) Chemotaxis of REH cells to the CXCR3 ligand CXCL10, $5x10^6$ cells were washed and re-suspended in chemotaxis buffer (RPMI 1640 with 5 mg/ml BSA) and placed in the upper chamber of a transwell assay (5µM transwell filters, Corning). Chemotaxis buffer +/- 300ng/ml CXCL10 was added to the bottom chamber. Following incubation for 3 h at 37^oC, 5% CO_2, transmigrated cells in the bottom well were counted using a haemocytometer with trypan blue dead-cell exclusion or by FACS analysis. Each condition was tested in triplicate wells. (b) Immunoassay for CXCL10 (Luminex, Invitrogen) was performed on CSF samples taken during induction therapy from one ALL patient with CNS-3 disease and 2 CNS-1 patients. (c) Immunohistochemical staining for the PSGL-1 receptor P-selectin using CD62P Antibody IHC-plus™ LS-B3578 (LifeSpan BioSciences) or isotype control in paraffin embedded sections of brain tissue from NSG mice showing meningeal covering and vessels within the meninges. A = meningeal arteriole, V = meningeal venule, P= Brain parenchyma

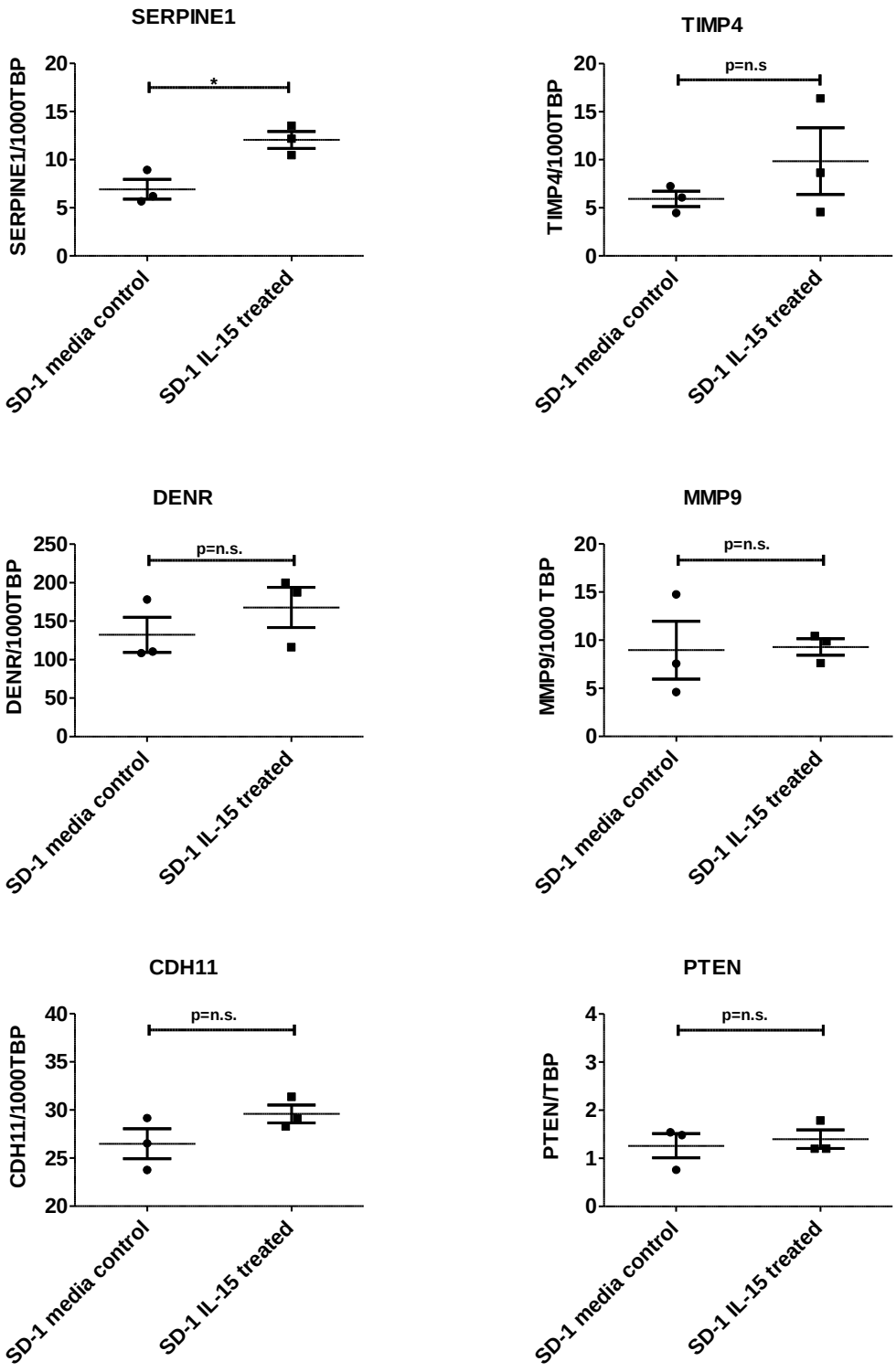

Figure S4: qPCR validation of possible IL-15 target genes using SYBR green absolute quantification. SD1 cells were treated with 25ng/ml IL-15 or media control for 72 hours. mRNA was extracted and cDNA synthesized and SYBR-green qPCR was performed using TATA binding protein as the housekeeping gene. The data is from 3 independent experiments each conducted in triplicates. Graph represents mean and SEM.

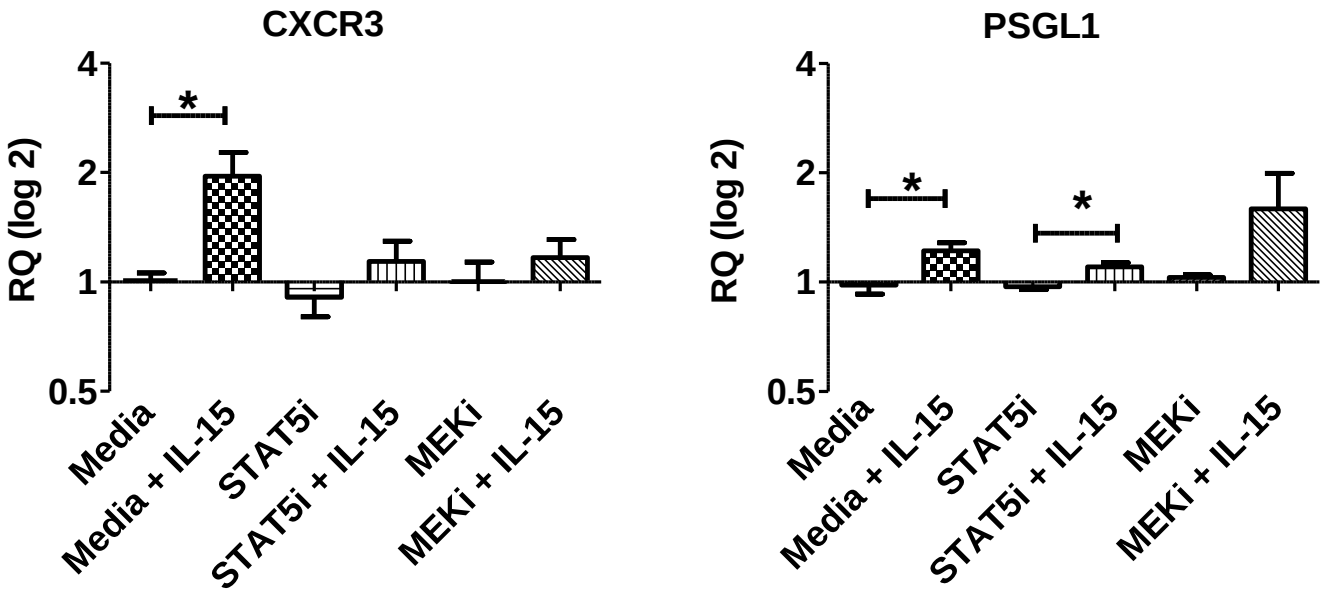

Figure S5: Effect of STAT5 and MEK inhibitors on the transcriptional response to IL-15. SD1 cells were treated with STAT5 inhibitor (573108, 10 µM) or MEK inhibitor (U0126, 1 µM) with or without IL15 (25ng/ml) in 10% FCS in RPMI for 72 hours. mRNA was extracted, cDNA synthesised. Gene expression was compared between media and IL-15 treated cells using Taqman gene expression assays for CXCR3 and PSGL1 using GAPDH as housekeeping gene. Data were analysed using 2ΔΔCT method on ABI RQ manager v1.2.1. Data is pooled from 3 independent experiments. Bars represent mean and SEM. *$p<0.05$